microstructure abnormalities in cortical bones and delayed fracture healing were observed [13, 14], in spite of the evident normal phenotype [15]. Also, bone loss after estrogen depletion was mitigated in IL-6-deficient mice, while a high level of IL-6 and bone loss are seen in wild-type mice [13]. Moreover, IL-6-overexpressed-transgenic mice develop osteopenia and defective ossification, in which the activity of mature osteoblasts is significantly decreased [16]. All these findings, together with studies on human RA patients [17, 18], indicate that IL-6 plays a major role in bone turnover and is an important regulator of bone homeostasis.

Recently, several biological agents have been introduced for the treatment of RA and have demonstrated not only potent anti-inflammatory effects but also inhibitory effects on joint destruction. Among these biological agents, tocilizumab, an anti-IL-6 receptor antibody, has been reported to increase serum bone formation markers in RA patients [19], suggesting that IL-6 has a negative effect on osteoblast differentiation. However, previous reports regarding the effects of IL-6 on osteoblast differentiation in vitro have been inconsistent [20]. IL-6 has been shown to decrease the expression of differentiation markers in osteoblasts [21, 22] and to inhibit bone formation [23], while it has been shown to induce osteoblast differentiation [24, 25].

Binding of IL-6 with sIL-6R or mIL-6R leads to subsequent homodimerization of the signal-transducing molecule gp130, followed by activation of two major intracellular signaling pathways, Janus protein tyrosine kinase (JAK)/signal transducer and activator of transcription factors (STAT) 3, or Src-homology domain 2 containing protein-tyrosine phosphatase (SHP2)/mitogen-activated protein kinase-extracellular signal–regulated kinase kinase (MEK)/mitogen-activated protein kinase (MAPK), also called extracellular signal-regulated kinase (ERK) [26]. There have been many reports in which the effects of IL-6 on JAK/STAT3 and SHP2/ERK signal transduction pathways have been studied in osteoblasts, though it is still controversial whether differentiation is enhanced by IL-6 [9, 20]. SHP2 can also form a tertiary complex with the scaffolding proteins Gab1/2 and the p85 subunit of phosphatidylinositol-3-kinase (PI3K) [27], which leads to activation of the Akt pathway. Several papers have so far reported that the PI3K/Akt pathway triggered by IL-6 plays important roles in various cells [28–32], but no reports have been published regarding the effect of IL-6 on this pathway in osteoblasts.

The purpose of this study was to clarify the effect of IL-6 on osteoblast differentiation in vitro, with consideration of intracellular signaling pathways in murine MC3T3-E1 osteoblastic cells and primary murine calvarial osteoblasts.

Materials and methods

Ethics statement

Prior to the study, all experimental protocols were approved by the Ethics Review Committee for Animal Experimentation of Osaka University School of Medicine.

Cell culture

MC3T3-E1 osteoblastic cells were purchased from Riken Cell Bank (Tsukuba, Japan). MC3T3-E1 cells were cultured in α-minimum essential medium (α-MEM) containing 10 % fetal bovine serum (FBS; Equitech-Bio, Kerrville, TX, USA) and 1 % penicillin and streptomycin at 37 °C in a humidified atmosphere of 5 % CO_2. All media were purchased from Life Technologies Japan (Tokyo, Japan). Murine primary osteoblasts were isolated from the calvariae of 3-day-old C57BL/6 mice (Charles River Laboratories Japan, Inc, Osaka, Japan) by sequential collagenase digestion as described previously [33].

MC3T3-E1 cells and murine calvarial osteoblasts were seeded at 1×10^5 cells per well in 12-well plates. After the cells reached confluence, the medium was replaced to induce osteoblast differentiation. The differentiation medium contained 10 % FBS, 10 mM β-glycerophosphate, and 50 μg/ml ascorbic acid in the absence or presence of recombinant mouse (rm) IL-6 (R&D Systems, Inc., Minneapolis, MN, USA) (10, 50 ng/mL), and rm sIL-6R (R&D Systems) (100 ng/mL). The medium and reagents were renewed every 3 days.

To study signal transduction, the following inhibitors or vehicle (DMSO) (Sigma-Aldrich, St.Louis, MO, USA) were added to culture medium at several concentrations; MEK inhibitor (U0126; 1, 2.5, 5 μM; Cell Signaling Technology, Danvers, MA, USA), STAT3 inhibitor (V Stattic; 2.5, 5 μM; Calbiochem, La Jolla, CA, USA), PI3K inhibitor (LY294002; 1, 2.5, 5 μM; Cell Signaling Technology), and SHP2 inhibitor (PHPS1; 5, 20, 40 μM; Sigma-Aldrich). These inhibitors were added 1 h before treatment with IL-6/sIL-6R. All inhibitors were maintained until the end of the culture period at the indicated concentrations.

Alkaline phosphatase (ALP) staining and activity

MC3T3-E1 cells and murine calvarial osteoblasts were treated with or without IL-6/sIL-6R and signal pathway inhibitors after the cells reached confluence and were incubated for 6 days.

For ALP staining, after fixation with 10 % formalin, cells were washed twice with phosphate-buffered saline (PBS) (pH 7.4) and incubated with ALP substrate solution,

0.1 mg/ml naphthol AS-MX (Sigma-Aldrich), and 0.6 mg/ml fast violet B salt (Sigma-Aldrich) in 0.1 M Tris–HCl (pH 8.5) for 20 min.

To measure ALP activity, cells were washed twice with PBS and lysed in Mammalian Protein Extraction Reagent (Pierce, Rockford, IL, USA) according to the manufacturer's protocol. ALP activity was assayed using *p*-nitrophenylphosphate as a substrate by an Alkaline Phosphatase Test Wako (Wako Pure Chemicals Industries, Ltd., Osaka, Japan), and the protein content was measured using the Bicinchoninic Acid Protein Assay Kit (Pierce).

Proliferation assay

MC3T3-E1 cells were cultured in 96-well plates at a concentration of 2.0×10^4 cells/cm^2 in α-MEM containing 10 % FBS. Cells were incubated for 1 day, after which the medium was treated with IL-6/sIL-6R for 3 days. Cell proliferation was assessed using the Premix WST-1 Cell Proliferation Assay System (Takara Bio, Inc., Otsu, Japan) according to the manufacturer' s instructions. We performed this assay every 24 h.

Alizarin red staining

After fixation with 10 % formalin, MC3T3-E1 cells and murine calvarial osteoblasts were washed with distilled water, and stained with alizarin red S solution (Sigma-Aldrich) (pH 6.0) for 10 min, followed by incubation in 100 mM cetylpyridinium chloride for 1 h at room temperature to dissolve and release calcium-bound alizarin red. The absorbance of the released alizarin red was then measured at 570 nm [34]. To measure the value of absorbance for alizarin red, the absorbance data were normalized by total DNA content. Total DNA was extracted using a DNeasy Blood & Tissue Kit (Qiagen, Düsseldorf, Germany).

Knockdown of MEK1, MEK2, Akt1 and Akt2 using RNA interference

MC3T3-E1 cells were transfected with small interfering RNAs (siRNA) using Lipofectamine RNAiMAX (Life Technologies Japan) according to the reverse transfection method in the manufacturer's protocol.

The siRNAs for MEK2, Akt1 and Akt2 and that for MEK1 were purchased from Cell Signaling Technology and Qiagen, respectively, with negative controls for each molecule. MC3T3-E1 cells transfected with siRNA were seeded in 24-well plates at a concentration of 1.0×10^4 cells/cm^2 for 48 h. The medium was then replaced with differentiation medium with vehicle or with 20 ng/ml IL-6 and 100 ng/ml sIL-6R and the cells were incubated for 3 days prior to use for further experiments.

Western blotting

Cells cultured in 6-well plates for 2 days were washed twice with PBS and then homogenized with 100 μl of Kaplan buffer (150 mM NaCl, 50 mM Tris–HCL pH 7.4, 1 % NP40, 10 % glycerol, and 1 tablet per 50 ml buffer of protease inhibitor cocktail and phosphatase inhibitor cocktail). The lysates were centrifuged at 13,000 rpm for 20 min at 4 °C, and the supernatants were used for electrophoresis after a protein assay using bovine serum albumin as standard. Western blotting was performed by use of the following antibodies purchased from Cell Signaling Technology, except for phosphate anti-Akt2 antibody from Enogene Biotech (New York, NY, USA): phosphate anti-STAT3 (Tyr705) (1:2000) and anti-STAT3 (1:1000); phosphate anti-Akt (Ser473) (1:2000), phosphate anti-Akt2 (Ser474) (1:1000), anti-Akt1, anti-Akt2, and anti-Akt (1:1000); phosphate anti-ERK (Thr202/Tyr204) (1:2000), anti-MEK1, anti-MEK2 and anti-ERK (1:1000); and phosphate anti-SHP2 (Tyr542) (1:1000). To control for protein loading, blots were additionally stained with anti-β actin antibody (1:1000).

Reverse transcription polymerase chain reaction (RT–PCR)

Total RNA was extracted from cells with an RNeasy Mini Kit (Qiagen), and first-strand cDNA was synthesized using SuperScript II RNase H-reverse transcriptase (Life Technologies Japan). Then PCR was performed using Ex Taq (Takara Bio) and the following primers:

Osteocalcin (forward primer 5′-CTCACTCTGCTGGCCCTG-3′; reverse primer 5′-CCGTAGATGCGTTTGTAGGC-3′);
Osterix (forward primer 5′-AGGCACAAAGAAGCCATAC-3′; reverse primer 5′-AATGAGTGAGGGAAGGGT-3′);
Runx2 (forward primer 5′-GCTTGATGACTCTAAACCTA-3′; reverse primer 5′-AAAAAGGGCCCAGTTCTGAA-3′);
GAPDH (forward primer 5′-TGAACGGGAAGCTCACTGG-3′; reverse primer 5′-TCCACCACCCTGTTGCTGTA-3′).

Quantitative real-time PCR analysis

We obtained cDNA by reverse transcription as mentioned above, and proceeded with real-time PCR using a Light Cycler system (Roche Applied Science, Basel, Switzerland). The SYBR Green assay using a Quantitect SYBR Green PCR Kit (Qiagen), in which each cDNA sample was evaluated in triplicate 20-μl reactions, was used for all

target transcripts. Expression values were normalized to GAPDH.

Statistical analysis

The results are expressed as the mean ± standard error (SE). Between-group differences were assessed using the ANOVA test. A probability value of <0.05 was considered to indicate statistical significance.

Results

IL-6/sIL-6R does not affect proliferation, but significantly reduces ALP activity and expression of osteoblastic genes in MC3T3-E1 cells

We first measured the proliferation of MC3T3-E1 cells with IL-6. Cell proliferation did not show significant difference in any culture condition (Fig. 1a).

To investigate the influence of IL-6 treatment on osteoblast differentiation, we examined ALP activity in MC3T3-E1 cells. As shown in Fig. 1b and c, IL-6/sIL-6R significantly reduced ALP activity in a dose-dependent manner. The single addition of sIL-6R did not show a significant difference as compared to the negative control with vehicle. As shown in Fig. 1d and e, gene expression of Runx2, osterix and osteocalcin was significantly downregulated by IL-6/sIL-6R in a dose-dependent manner. Again, the single addition of sIL-6R did not show significant difference as compared to the negative control with vehicle.

IL-6/sIL-6R significantly inhibits mineralization of extracellular matrix (ECM) in MC3T3-E1 cells

As shown in Fig. 2a, IL-6/sIL-6R significantly inhibited the mineralized area in a dose-dependent manner. The single addition of sIL-6R did not show a significant difference as compared to the negative control with vehicle (Fig. 2a). Quantitative analysis of mineralization by measuring the absorbance of alizarin red revealed a significant decrease by IL-6/sIL-6R in a dose-dependent manner (Fig. 2b).

IL-6/sIL-6R activates ERK, STAT3 and Akt2 signal transduction pathways in MC3T3-E1 cells

When MC3T3-E1 cells were incubated in the presence of IL-6/sIL-6R, phosphorylation of ERK, STAT3 and Akt was clearly observed at 15 min, and their activation became weaker at 30 min. When only sIL-6R was added, there was no apparent activation of ERK, STAT3, or Akt as compared to the negative control (Fig. 3a). As for Akt, the phosphorylation by IL-6/sIL-6R was recognized more strikingly as early as 5 min in a dose-dependent manner, both for whole and for Akt2 only, one of its three isoforms (Fig. 3b).

IL-6-induced activation of ERK is enhanced by blocking the STAT3 signaling pathway, and IL-6-induced ERK and Akt signaling pathways negatively regulate each other reciprocally

The SHP2 inhibitor PHPS1 [35] inhibited IL-6-induced phosphorylation of ERK and Akt to the constitutive level, but did not inhibit STAT3 (Fig. 4a and Supplementary Fig. S1a), suggesting that the downstream pathways of SHP2 are ERK and Akt, not STAT3. The STAT3 inhibitor V Stattic inhibited the phosphorylation of STAT3 but enhanced ERK significantly (Fig. 4a and Supplementary Fig. S1a), suggesting that STAT3 could negatively regulate ERK, which is consistent with previous reports [36]. The MEK/ERK inhibitor U0126 completely inhibited both constitutive and IL-6-induced phosphorylation of ERK but enhanced those of Akt. Moreover, the PI3K/Akt inhibitor LY294002 completely inhibited both constitutive and IL-6-induced phosphorylation of Akt but enhanced those of ERK (Fig. 4b and Supplementary Fig. S1b). From these findings, we concluded that IL-6-induced ERK and Akt signaling pathways, both of which are downstream of SHP2, can negatively regulate each other reciprocally.

The negative effects of IL-6 on osteoblast differentiation are restored by inhibition of MEK, PI3K and SHP2, while they are enhanced by inhibition of STAT3

To identify the intracellular signaling pathways associated with the downregulation of osteoblast differentiation, the effects of various signal transduction inhibitors, consisting of a MEK inhibitor (U0126), PI3K inhibitor (LY294002), SHP2 inhibitor (PHPS1), and STAT3 inhibitor (V Stattic), were assessed for ALP activity, the expression of osteoblastic genes (Runx2, osterix and osteocalcin), and the mineralization of ECM.

The negative effect of IL-6/sIL-6R on ALP activity was restored by treatment with either U0126, LY294002, or PHPS1 in a dose-dependent manner. On the other hand, the negative effect of IL-6/sIL-6R on ALP activity was enhanced by treatment with V Stattic (Fig. 5a). These results indicate that the SHP2-associated signal transduction molecules MEK/ERK and PI3K/Akt have a negative effect on osteoblast differentiation, whereas the JAK-associated molecule STAT3 has a positive effect.

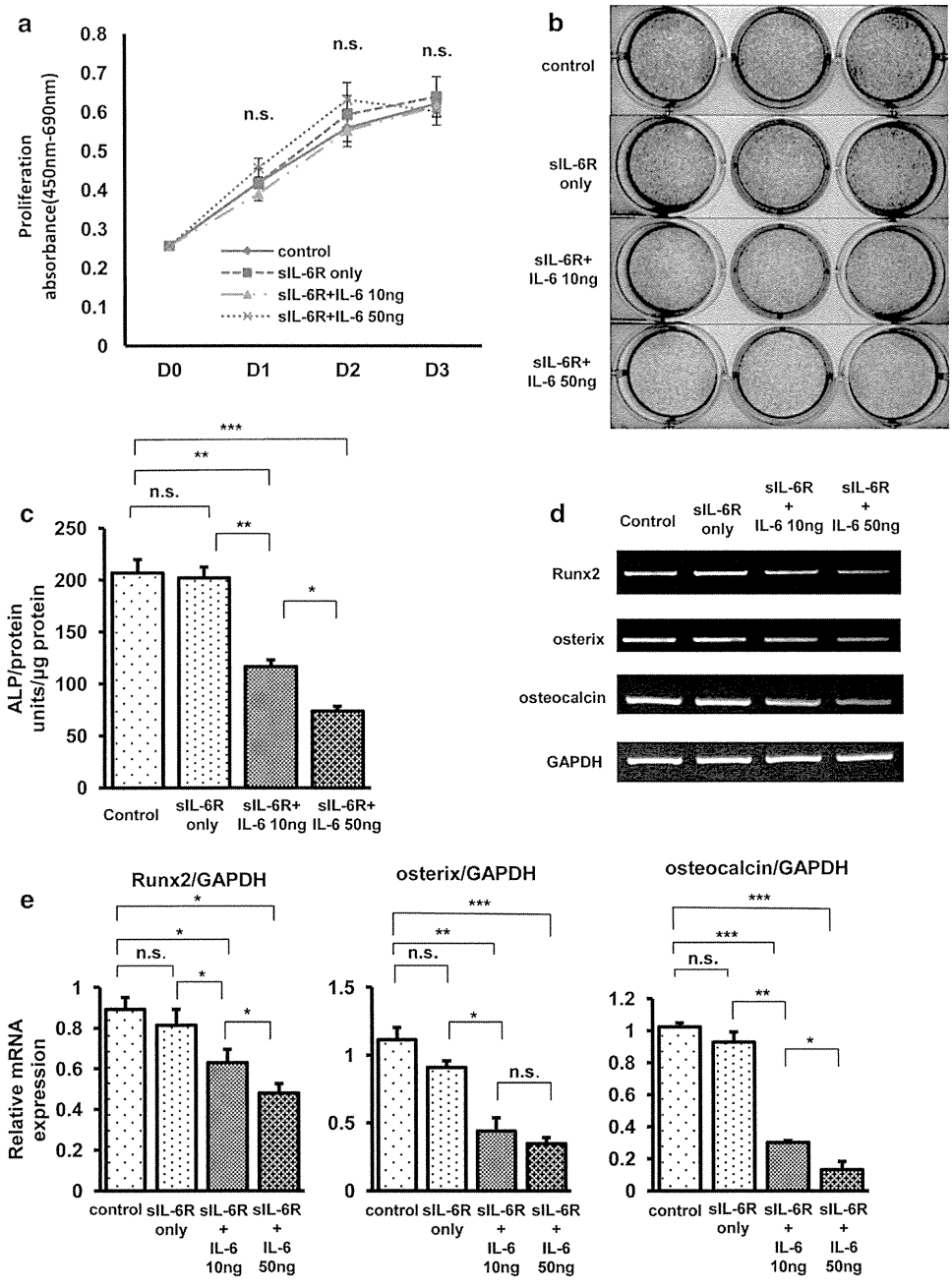

Fig. 1 IL-6/sIL-6R significantly reduced ALP activity and expression of osteoblastic genes in MC3T3E1 cells, but did not affect proliferation. **a** Proliferation of MC3T3-E1 cells with IL-6/sIL-6R was examined. Cells were pre-incubated for 1 day and then the medium was treated with or without IL-6/sIL-6R for 3 days. Cell proliferation assay was performed daily throughout the 4 days of incubation. Cell proliferation did not show significant differences in any culture condition. **b** ALP staining was performed in MC3T3-E1 cells treated with or without IL-6/sIL-6R for 6 days. Apparently significant reduction of ALP staining was recognized in cells treated with either 10 or 50 ng/ml IL-6. **c** ALP activity of the lysates of MC3T3-E1 cells treated with or without IL-6/sIL-6R for 6 days was measured using p-nitrophenylphosphate as a substrate. IL-6/sIL-6R significantly reduced ALP activity in a dose-dependent manner. **d** Total RNA was extracted from MC3T3-E1 cells treated with or without IL-6/sIL-6R for 6 days and subjected to RT-PCR for osteoblastic genes Runx2, osterix, and osteocalcin. Apparently significant reduction of osteoblastic gene expression was recognized in cells treated with either 10 or 50 ng/ml IL-6. **e** Real-time PCR for Runx2, osterix, and osteocalcin was performed for quantitative analysis. Data were normalized to GAPDH expression and are shown as the ratio of expression compared to control cells treated with vehicle. The expression of osteoblastic genes was significantly downregulated by IL-6/sIL-6R in a dose-dependent manner. Representative data from at least 3 independent experiments are shown. Data are shown as mean ± SE. *n.s.* not significant; $*P < 0.05$; $**P < 0.001$; $***P < 0.001$

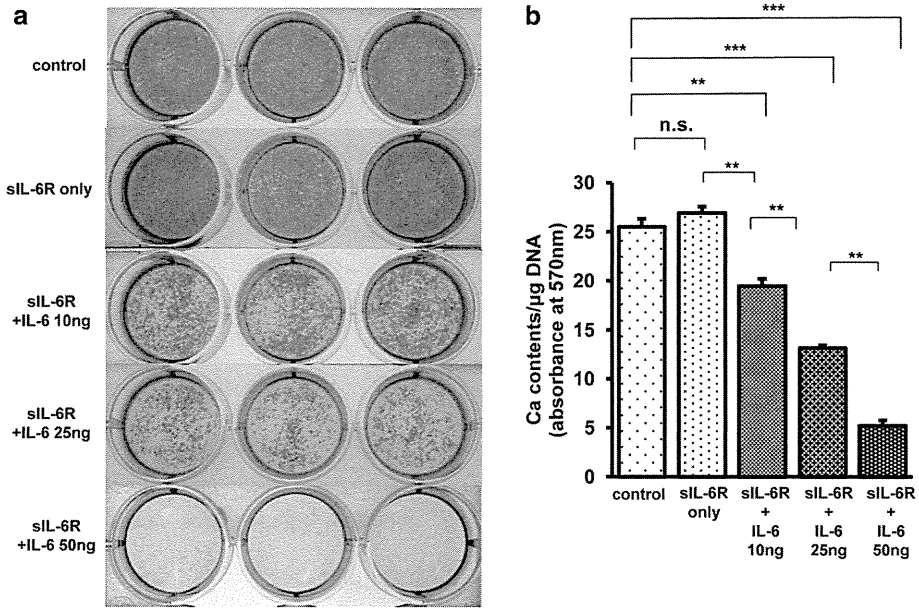

Fig. 2 IL-6/sIL-6R significantly inhibited the mineralization of ECM in MC3T3E1 cells. MC3T3-E1 cells were treated with or without IL-6/sIL-6R and were incubated for 21 days. **a** After fixation, the cells were stained with alizarin red solution. Apparently significant reduction of alizarin red staining was recognized in the cells treated with either 10, 25, or 50 ng/ml IL-6. **b** Matrix mineralization was quantified by the measurement of absorbance of alizarin red and normalized by total DNA content. Matrix mineralization was significantly reduced by IL-6/sIL-6R in a dose-dependent manner. Representative data from at least 3 independent experiments are shown. Data are shown as mean ± SE. *n.s.* not significant; $*P < 0.05$; $**P < 0.001$; $***P < 0.001$

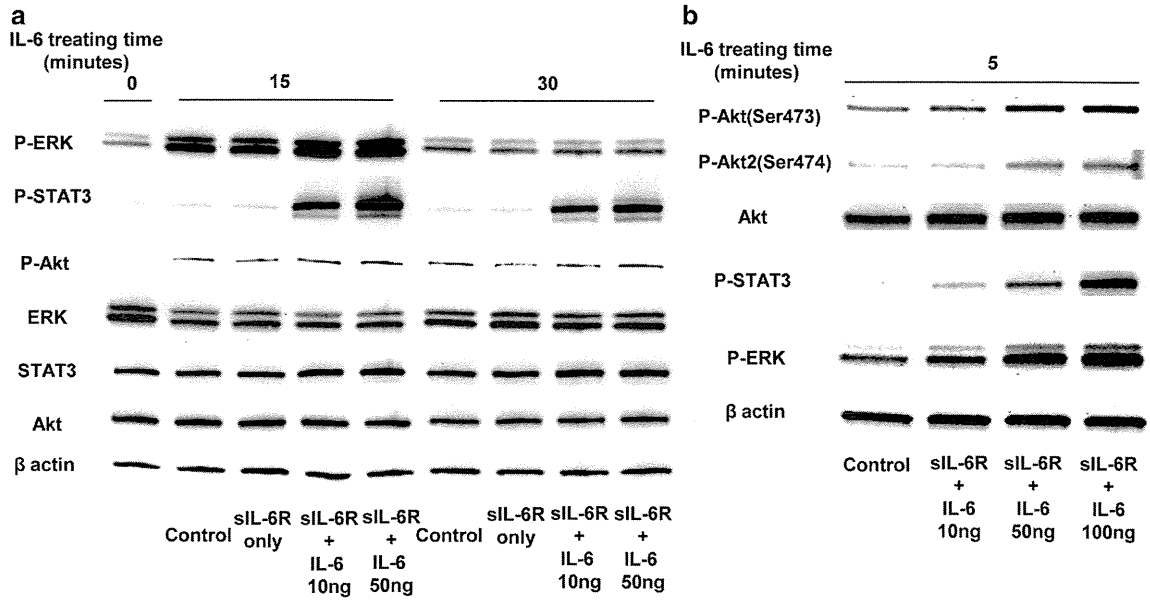

Fig. 3 IL-6/sIL-6R-activated ERK, STAT3, and Akt2 signal transduction pathways in MC3T3-E1 cells. **a** MC3T3-E1 cells were treated with vehicle or with 10 or 50 ng/ml IL-6 and 100 ng/ml sIL-6R in a time-course experiment (0, 15, and 30 min). Western blot analysis was performed using cell lysates for the detection of ERK, STAT3, and Akt, either phosphorylated or not. IL-6/sIL-6R significantly induced the phosphorylation of ERK, STAT3, and Akt in a dose-dependent manner. **b** MC3T3-E1 cells were incubated with increasing concentrations of IL-6 and 100 ng/ml sIL-6R for 5 min. Western blotting was performed using cell lysates for the detection of ERK, STAT3, as well as Akt, either non-phosphorylated, phosphorylated, or the phosphorylated isoform Akt2. The phosphorylation of both whole Akt and Akt2 by IL-6/sIL-6R was recognized more strikingly in a dose-dependent manner. Representative data from at least three independent experiments are shown

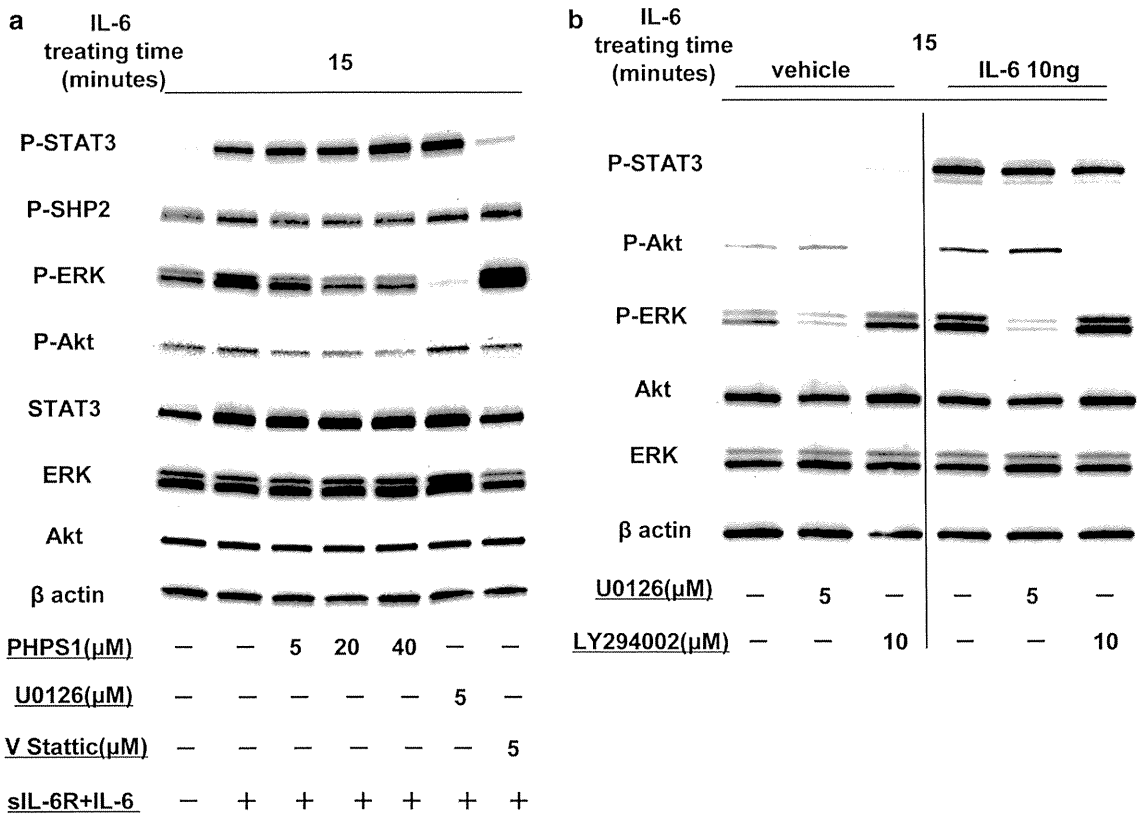

Fig. 4 IL-6-induced activation of ERK was enhanced by blocking the STAT3 signaling pathway, and IL-6-induced ERK and Akt signaling pathways negatively regulated each other reciprocally. **a** MC3T3-E1 cells were stimulated with 10 ng/ml IL-6 and 100 ng/ml sIL-6R (15 min) after pretreatment either with PHPS1 (5, 20, 40 μM; 1 h), with U0126 (5 μM; 1 h), or with V Stattic (5 μM; 1 h), and the cell lysates were subjected to Western blotting. PHPS1 inhibited IL-6-induced phosphorylation of ERK and Akt to the constitutive level, but not of STAT3. IL-6-induced activation of ERK was enhanced by V Stattic. **b** MC3T3-E1 cells were treated with vehicle or with 10 ng/ml IL-6 and 100 ng/ml sIL-6R (15 min) after pretreatment either with U0126 (5 μM; 1 h) or with LY294002 (10 μM; 1 h), and the cell lysates were subjected to Western blotting. Both constitutive and IL-6-induced phosphorylation of Akt and ERK were enhanced by treatment with U0126 and LY294002, respectively. Representative data from at least three independent experiments are shown

The negative effect of IL-6/sIL-6R on the expression of osteoblastic genes (Runx2, osterix and osteocalcin) was also restored by treatment with either U0126, LY294002, or PHPS1 in a dose-dependent manner, while it was enhanced by treatment with V Stattic (Fig. 5b). Moreover, a high dose of PHPS1, 20 μM, caused significantly upregulated expression of osteocalcin.

For mineralization of ECM, the negative effect of IL-6/sIL-6R was restored by treatment with either U0126, LY294002, or PHPS1. As with ALP activity and osteoblastic gene expression, the negative effect of IL-6/sIL-6R on mineralization was enhanced by treatment with V Stattic (Fig. 6a, b). ALP activity, osteoblastic gene expression, and mineralization of ECM in cells treated only with each inhibitor demonstrated the same behavior (Figs. 5, 6).

Furthermore, the negative effects of ALP activity, osteoblastic gene expression and mineralization of ECM by stimulation with IL-6/sIL-6R were compared for levels in the presence and in the absence of each inhibitor. The negative effects on osteoblast differentiation by IL-6/sIL-6R showed a tendency to decrease in the presence of each inhibitor, as compared to the absence of inhibitors (Figs. 5, 6). The negative effects were decreased by 15–44, 20–61, 7–140, and 21–80 % in the presence of U0126, LY294002, PHPS1 and V Stattic, respectively, as compared to the absence of inhibitors. These results indicate that the effects of IL-6/sIL-6R on osteoblast differentiation might be mediated either by MEK/ERK, PI3K/Akt, or JAK/STAT3 pathways.

Knockdown of MEK2 and Akt2 via siRNA transfection restores ALP activity and Runx2 gene expression

To further confirm the effects of MEK and Akt inhibition on osteoblast differentiation in MC3T3-E1 cells, we studied cell differentiation after knockdown of MEK and Akt. For each protein, RNAs of two isoforms were separately blocked: MEK1 and MEK2 for MEK, and Akt1 and Akt2 for Akt.

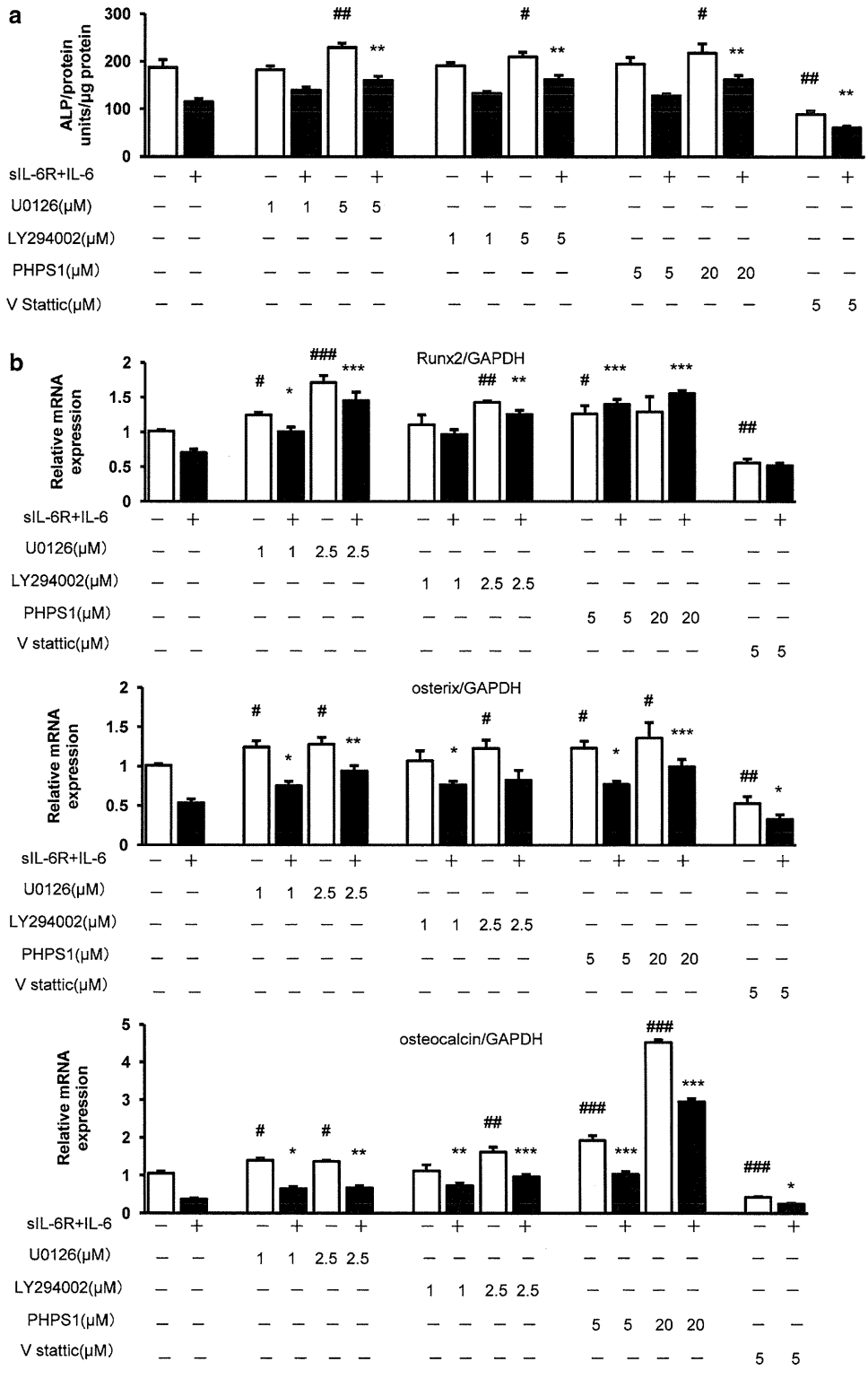

Fig. 5 The negative effects of IL-6 on ALP activity and the expression of osteoblastic genes were restored by inhibition of MEK, PI3K, and SHP2, while they were enhanced by inhibition of STAT3. MC3T3-E1 cells were pretreated either with U0126 (1, 2.5, 5 μM; 1 h), LY294002 (1, 2.5, 5 μM; 1 h), PHPS1 (5, 20 μM; 1 h), or V Stattic (5 μM; 1 h), then stimulated either with 10 ng/ml IL-6 and 100 ng/ml sIL-6R or with vehicle and incubated for 6 days. (a) ALP activity of the cell lysates was measured using p-nitrophenylphosphate as a substrate. The negative effect of IL-6 on ALP activity was restored by treatment with either U0126, LY294002, or PHPS1 in a dose-dependent manner, while it was enhanced by treatment with V Stattic. **b** Total RNA was extracted and real-time PCR for Runx2, osterix, and osteocalcin was performed. Data were normalized to GAPDH expression and are shown as the ratio of gene expression compared to control cells treated with vehicle. The negative effect of IL-6 on expression of osteoblastic genes was restored by treatment either with U0126, LY294002, or PHPS1 in a dose-dependent manner, while it was enhanced by treatment with V Stattic. Representative data from at least three independent experiments are shown. Data are shown as mean ± SE. *n.s.* not significant; $^{\#}P < 0.05$; $^{\#\#}P < 0.001$; $^{\#\#\#}P < 0.001$, compared to the group treated with vehicle. $^{*}P < 0.05$; $^{**}P < 0.001$; $^{***}P < 0.001$, compared to group treated with IL-6/sIL-6R

The protein expression level of each molecule was found to be diminished selectively at 48 h after transfection of the respective siRNAs (Fig. 7a). The ALP activity in MC3T3-E1 cells treated with IL-6/sIL-6R was restored by knockdown of MEK2 and Akt2 as compared to that in cells transfected with negative control siRNA. On the other hand, knockdown of MEK1 and Akt1 enhanced the negative effects of IL-6/sIL-6R on ALP activity (Fig. 7b) (ALP activity after transfection with each siRNA without IL-6/sIL-6R demonstrated the same behavior; Fig. 7b) Quantitative real-time PCR analysis revealed that the gene expressions of Runx2, osterix, and

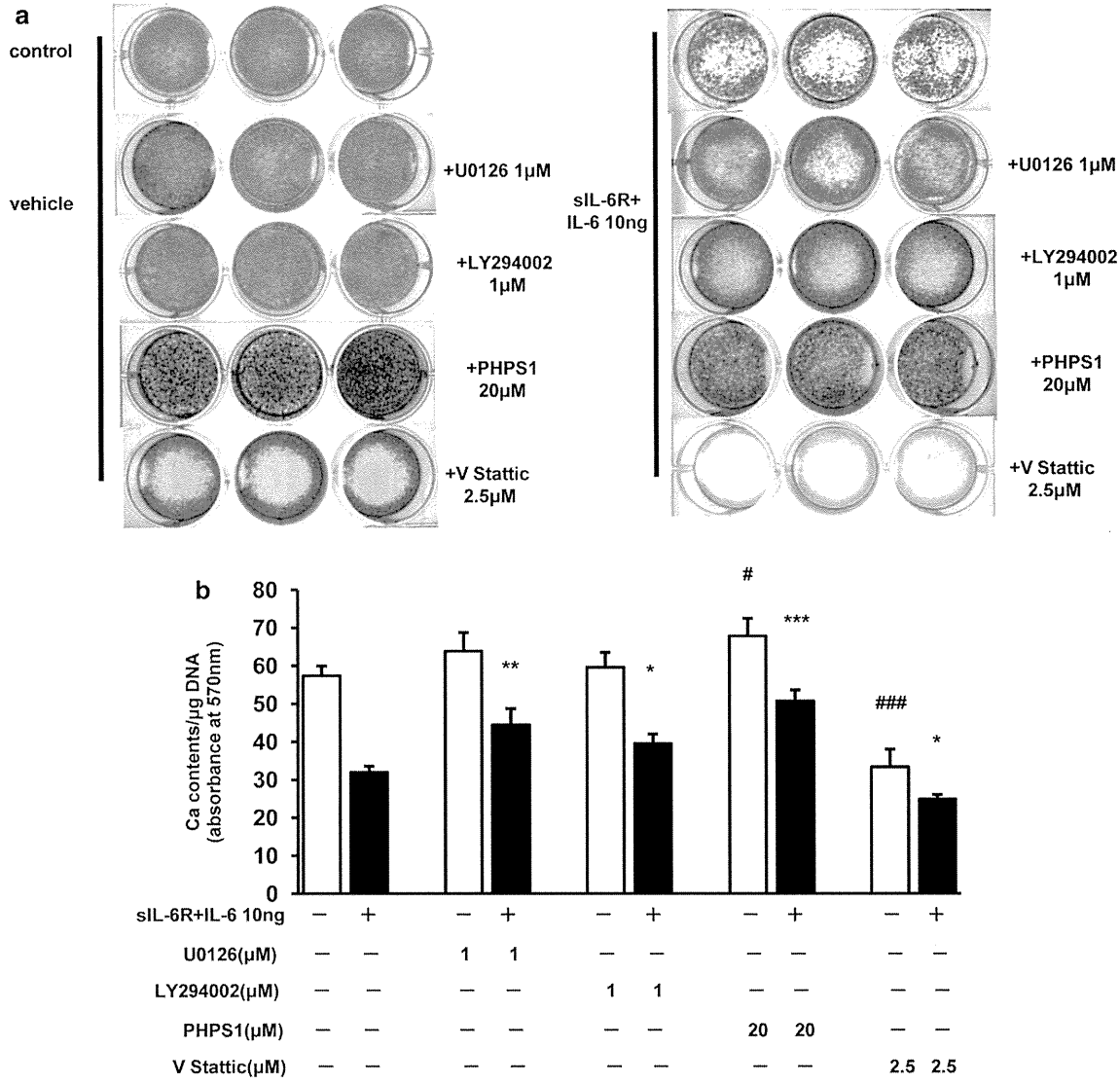

Fig. 6 The negative effect of IL-6 on mineralization of ECM was restored by inhibition of MEK, PI3K, and SHP2, while it was enhanced by inhibition of STAT3. MC3T3-E1 cell were pretreated either with U0126 (1 μM; 1 h), LY294002 (1 μM; 1 h), PHPS1 (20 μM; 1 h), or V Stattic (2.5 μM; 1 h), then stimulated with either 10 ng/ml IL-6 and 100 ng/ml sIL-6R or with vehicle and incubated for 21 days. **a** After fixation, the cells were stained with alizarin red solution. The reduction of alizarin red staining by IL-6/sIL-6R was restored in cells treated with either U0126, LY294002, or PHPS1, while it was enhanced in those treated with V Stattic. **b** Quantification of matrix mineralization was by measurement of absorbance for alizarin red normalized by total DNA content. The reduction of matrix mineralization by IL-6/sIL-6R was restored in cells treated with either U0126, LY294002, or PHPS1, while it was enhanced in those treated with V Stattic. Representative data from at least three independent experiments are shown. Data are shown as mean ± SE. *n.s.* not significant; $^{\#}P < 0.05$; $^{\#\#}P < 0.001$; $^{\#\#\#}P < 0.001$, compared to the group treated with vehicle. $^{*}P < 0.05$; $^{**}P < 0.001$; $^{***}P < 0.001$, compared to group treated with IL-6/sIL-6R

osteocalcin were restored by knockdown of MEK2. On the other hand, knockdown of Akt2 also restored Runx2, but decreased osteocalcin expression (Fig. 7c), while knockdown of Akt2 without IL-6/sIL-6R caused no significant difference in Runx2 expression (Fig. 7b). As was recognized for ALP activity, knockdown of MEK1 and Akt1 enhanced the downregulation of osteocalcin expression (Fig. 7b, c). Also, the negative effects of IL-6/sIL-6R on osteoblast differentiation showed some tendency to decrease with each knockdown compared to those without knockdown. The negative effects were decreased by 2–24, 4–27, 7–43, and 21–26 % with knockdown of MEK1, MEK2, Akt1, and Akt2, respectively, as compared to those without knockdown. These results indicate that IL-6 may suppress osteoblast differentiation through MEK2 and Akt2.

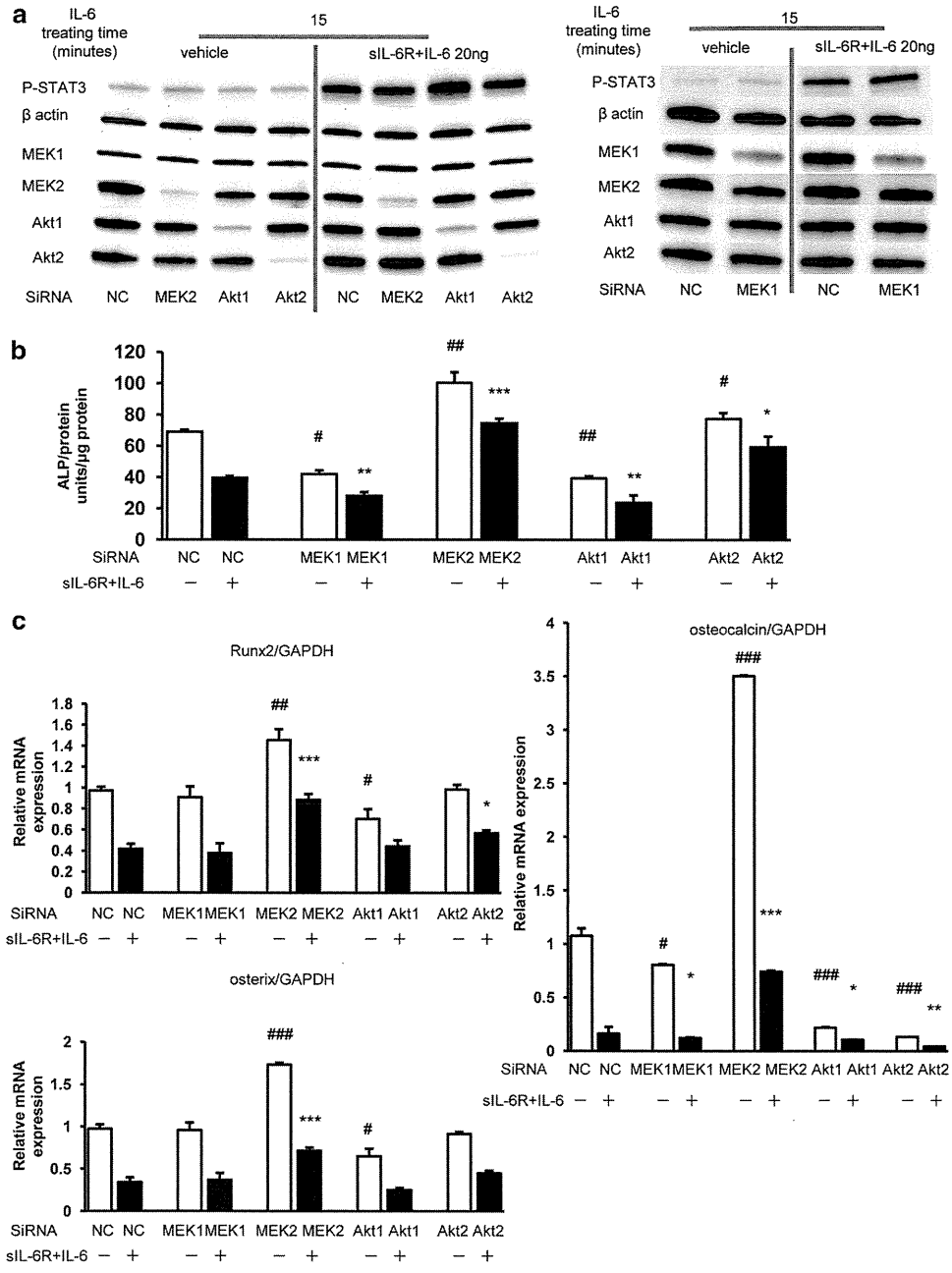

Fig. 7 Knockdown of MEK2 and Akt2 in cells transfected with siRNA restored ALP activity and Runx2 gene expression. **a** MC3T3-E1 cells transfected with respective siRNAs were cultured for 48 h. Western blotting was performed using cell lysates stimulated with vehicle or with 20 ng/ml IL-6 and 100 ng/ml sIL-6R (15 min). Expression levels of each protein, MEK1, MEK2, Akt1, and Akt2, were selectively diminished at 48 h after transfection with respective siRNAs. **b** MC3T3-E1 cells transfected with respective siRNAs were incubated for 48 h after which the medium was changed to differentiation medium with vehicle or with 20 ng/ml IL-6 and 100 ng/ml sIL-6R. The cells were then incubated for 3 days to evaluate osteoblast differentiation. ALP activity in MC3T3-E1 cells treated with IL-6/sIL-6R was restored by knockdown of MEK2 and Akt2 as compared to that in cells transfected with negative control siRNA. **c** Expression of osteoblastic genes in MC3T3-E1 cells transfected with respective siRNAs was assessed by real-time PCR. The expression of each gene was normalized against GAPDH expression. The gene expressions of Runx2, osterix, and osteocalcin were restored by knockdown of MEK2. Knockdown of Akt2 also restored Runx2, but decreased osteocalcin. Representative data from at least three independent experiments are shown. Data are shown as mean ± SE. *n.s.* not significant; $^{\#}P < 0.05$; $^{\#\#}P < 0.001$; $^{\#\#\#}P < 0.001$, compared to negative control group treated with vehicle. $^{*}P < 0.05$; $^{**}P < 0.001$; $^{***}P < 0.001$, compared to negative control group treated with IL-6/sIL-6R

IL-6/sIL-6R inhibits the differentiation of primary murine calvarial osteoblasts by activating phosphorylation of ERK, Akt2, and STAT3

Experiments were repeated with murine calvarial osteoblasts isolated from the calvariae of 3-day-old C57BL/6 mice. As was recognized in MC3T3-E1 cells, IL-6 inhibited ALP activity (Fig. 8a), the expression of osteoblastic genes (Fig. 8b), and mineralization (Fig. 8c, d) in a dose-dependent manner. Furthermore, IL-6 induced phosphorylation of ERK, Akt2, and STAT3 (Fig. 8e), which was exactly the same as with MC3T3-E1 cells.

Discussion

We examined the effects of IL-6 and its soluble receptor on the proliferation and differentiation of murine MC3T3-E1 osteoblastic cells and primary murine calvarial osteoblasts. Our results showed that they significantly reduced ALP activity, bone mineralization, and expression of the osteoblastic genes Runx2 osterix and osteocalcin, in a dose-dependent manner. From these experiments, we clearly demonstrated that IL-6 inhibited osteoblast differentiation of MC3T3-E1 cells and primary murine calvarial osteoblasts.

It has been demonstrated that the JAK/STAT3 signaling pathway has important roles both, in vivo and in vitro, in the differentiation of osteoblasts [37, 38]. Our results are consistent with previous reports and imply that the activation of STAT3 induced by IL-6 may induce osteoblast differentiation.

IL-6 activates another major intracellular signaling pathway, SHP2/ERK, and can also lead to the activation of an additional signaling cascade involving SHP2/PI3K/Akt. IL-6-induced activation of PI3K and downstream protein kinase Akt/PKB has been reported to play important roles in the proliferation of prostate cancer cells [30, 31], hepatoma cells [32], and multiple myeloma cells [29]. They were also reported to associate with neuroendocrine differentiation of prostate cancer cells induced by IL-6 [32]. In this study, we focused on the PI3K/Akt pathway triggered by IL-6, because no reports have demonstrated the role of IL-6 in the activation of PI3K/Akt signaling pathway in osteoblasts. We have demonstrated for the first time that IL-6-induced activation of Akt2, one of the downstream pathways of SHP2, may be a key player in the negative regulation of osteoblast differentiation induced by IL-6. Among the three isoforms of Akt, Akt1 and Akt2 are highly expressed in osteoblasts [39]. Mice lacking Akt1, the major isoform in bone tissue, exhibit osteopenia [40, 41], and the impact of Akt1 deficiency in osteoblast differentiation and bone development have also been published [39, 42–44], all of which are consistent with our results showing that knockdown of Akt1 signaling by siRNA inhibited osteoblast differentiation. In contrast, Mukherjee et al. [44] reported enhanced osteogenic differentiation in the absence of Akt1 in cell lines. Moreover, they reported that Akt2 was required for BMP2-initiated osteoblast differentiation of cultured murine mesenchymal stem cells, but that Akt1 was dispensable in this assay [45], which is inconsistent with our results showing that knockdown of Akt2 signaling by siRNA promoted osteoblast differentiation. These discrepancies might be due to the difference between cell types, i.e. intramembranous (calvariae) cells and endochondral (long bones) cells.

In this study, gene expression of osteocalcin, a late osteoblastic differentiation marker, was upregulated by treatment with a PI3K/Akt inhibitor, but was downregulated by knockdown of both Akt1 and Akt2. Moreover, a complete blockade with a high dose (more than 10 μM) of the PI3K/Akt inhibitor conversely downregulated the expression of osteocalcin (data not shown). This discrepancy may be due to the difference between the temporary or partial blockade by the inhibitor and constitutive knockdown by siRNA. Since bone formation has been reported to increase without impairment of mineralization and resorption even in osteocalcin-deficient mice [46], the expression of osteocalcin may not directly affect bone formation.

We have previously reported that osteoblast differentiation was significantly promoted by MEK inhibitor in BMP-2-treated C2C12 cells and MC3T3-E1 cells [47]. Our findings in the present study are consistent with our previous report and others [47–49] at the point that IL-6-induced activation of ERK significantly downregulated osteoblast differentiation. In addition, our results suggest that there might be different roles in osteoblast differentiation between MEK1 and MEK2. Constitutively active expression of MEK1 has been reported to accelerate bone development both in vitro [50] and in vivo [51], which is consistent with the results showing that knockdown of MEK1 inhibited osteoblast differentiation in the present study. As for MEK2, there are no reports concerning its roles in osteoblast differentiation, and we are the first to demonstrate that MEK2 may also be a key player in the negative regulation of osteoblast differentiation induced by IL-6. The effects of an MEK inhibitor that inhibits both MEK1 and MEK2 on bone formation are still controversial [52]. These controversies might be due to different roles played between MEK1 and MEK2 in osteoblast differentiation, and the effects of MEK inhibitors could depend on which pathway is predominantly inhibited in each study.

With respect to intracellular signaling pathways, our results showed that IL-6 triggers three signaling pathways, one of which has a conflicting function with the others.

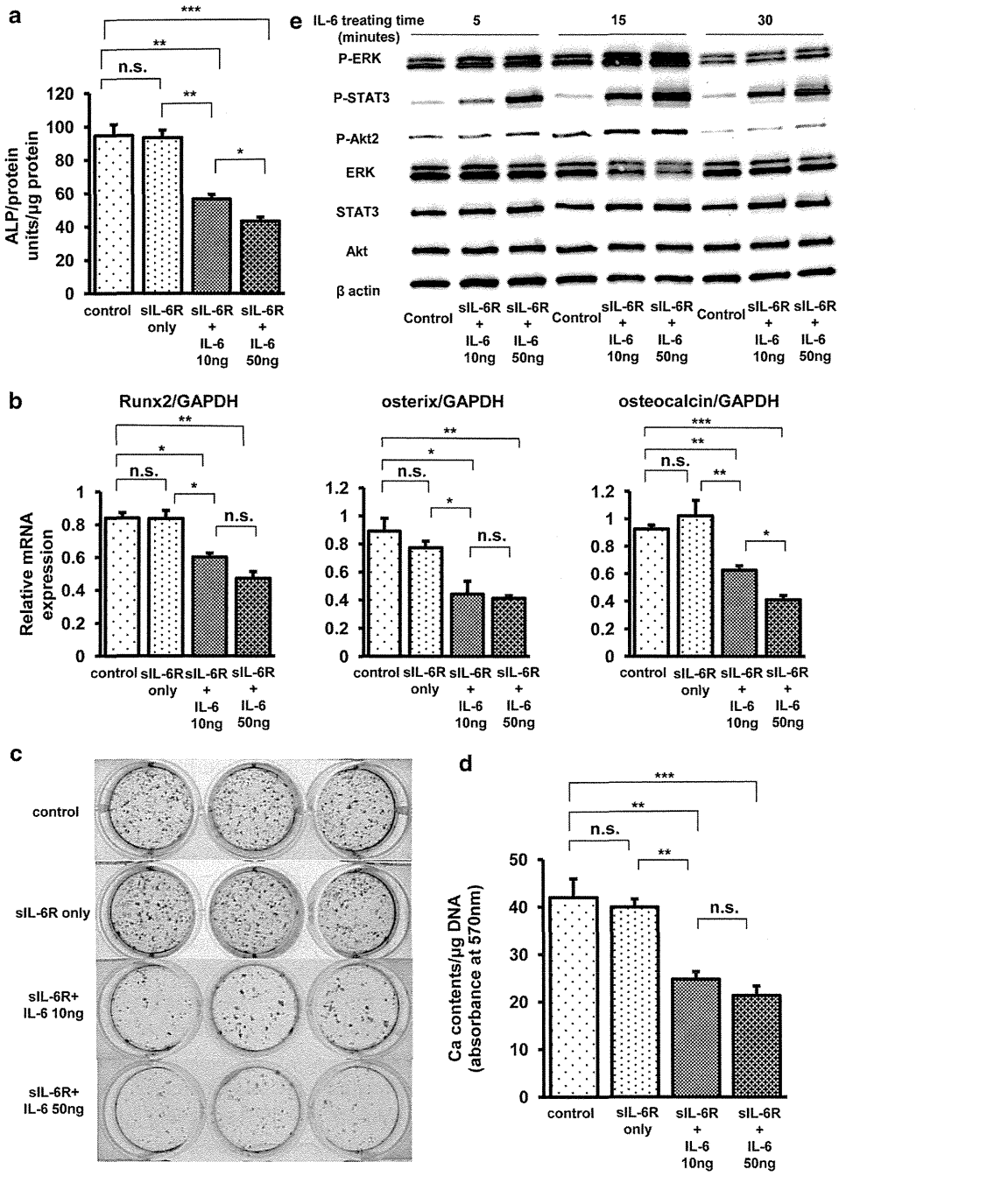

Fig. 8 IL-6/sIL-6R inhibited the differentiation of primary murine calvarial osteoblasts with the activated phosphorylation of ERK, Akt2, and STAT3. **a** ALP activity of lysates of murine calvarial osteoblasts treated with or without IL-6/sIL-6R for 6 days was measured using p-nitrophenylphosphate as a substrate. IL-6/sIL-6R significantly reduced ALP activity in a dose-dependent manner. **b** Total RNA was extracted from murine calvarial osteoblasts treated with or without IL-6/sIL-6R for 6 days, and real-time PCR for Runx2, osterix, and osteocalcin was performed. Data were normalized to GAPDH expression and are shown as the ratio of gene expression as compared to control cells treated with vehicle. The expression of osteoblastic genes was significantly downregulated by IL-6/sIL-6R in a dose-dependent manner. **c** Murine calvarial osteoblasts were treated with or without IL-6/sIL-6R and were cultured for 21 days. After fixation, the cells were stained with alizarin red solution. Apparently significant reduction of alizarin red staining was recognized in cells treated with either 10 or 50 ng/ml IL-6. **d** Matrix mineralization was quantified by measurement of absorbance for alizarin red normalized by total DNA content. IL-6/sIL-6R significantly inhibited mineralization of ECM in a dose-dependent manner. **e** Primary murine calvarial osteoblasts were treated with vehicle or 10 or 50 ng/ml IL-6 and 100 ng/ml sIL-6R in a time-course experiment (5, 15, and 30 min). Western blotting was performed using cell lysates. IL-6 significantly induced the phosphorylation of ERK, Akt2, and STAT3 in a dose-dependent manner. Representative data from at least three independent experiments are shown. Data are shown as mean ± SE. *n.s.* not significant; $*P < 0.05$; $**P < 0.001$; $***P < 0.001$

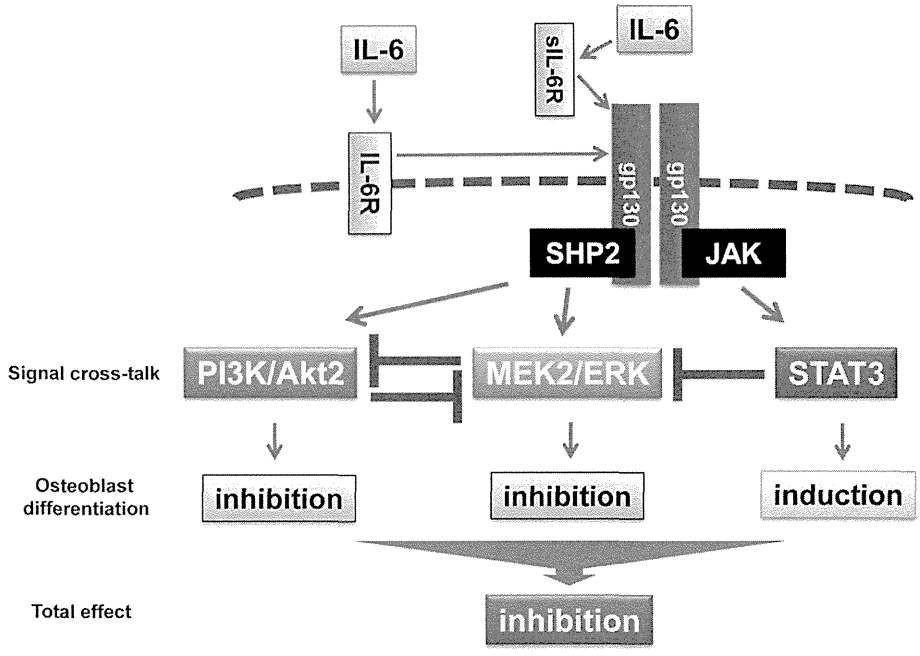

Fig. 9 Schematic presentation of signaling pathways involved in osteoblast differentiation induced by IL-6. IL-6-induced novel SHP2/MEK2/ERK and SHP2/PI3K/Akt2 signal crosstalk in osteoblastic cells; ERK and Akt signaling pathways, both of which are downstream of SHP2, negatively regulate each other reciprocally. On the other hand, the STAT3 signaling pathway negatively regulates the ERK signaling pathway. MEK2/ERK and PI3K/Akt2 have negative effects on osteoblast differentiation, whereas STAT3 has a positive effect. Overall, IL-6 inhibits osteoblast differentiation through MEK2 and Akt2 signaling pathways

SHP2/ERK and SHP2/Akt2 negatively affects osteoblast differentiation, whereas JAK/STAT3 positively affects it (Fig. 9). In other cells, it is often that simultaneous activation of the SHP2/ERK and JAK/STAT3 cascades generate opposing, or at least different signals. In osteoclasts, for example, SHP2/ERK activation inhibits osteoclastogenesis [53], whereas STAT3 is a pro-osteoclastic molecule after phosphorylation on serine727 [54]. In myeloid leukemic M1 cells, STAT3 induces differentiation in vitro [55], whereas the SHP2/ERK pathway promotes their proliferation [56]. These examples suggest that the integration of opposing activities transduced by more than one pathway could provide a biologically balanced state in the end, leaving availability to respond to another physiological situation. Indeed, Hirano and colleagues [57] have proposed a "signaling orchestration" model in a single cell, where the balance or interplay of simultaneously generated contradictory signals eventually determines the biological outcome. Thus, the inconsistent results regarding the effects of IL-6 on osteoblast differentiation in previous reports could be explained by which intracellular signaling pathway was predominantly activated in each study. The balance of three signaling pathways could be influenced by such conditions as the variety of cultured cells, the stage of cell differentiation, and the employed culture conditions.

To the best of our knowledge, this is the first report of signal crosstalk in which IL-6-induced ERK and Akt signaling pathways negatively regulated each other in cultured osteoblastic cells. In this study, however, cancellation of the negative effects of IL-6/sIL-6R on osteoblast differentiation by inhibitors was incomplete as compared to the absence of inhibitor (Figs. 5, 6). This might be because ERK, Akt and STAT3 are all critical pathways in osteoblast differentiation even in the absence of IL-6/sIL-6R, and even though one pathway is blocked, another pathway is enhanced by reciprocal regulation in the crosstalk between IL-6-activated signaling pathways (Fig. 9). Our results demonstrated that a STAT3 inhibitor significantly enhanced IL-6-induced activation of ERK and SHP2, but not of Akt (Fig. 4a). SHP2 could predominantly lead to the activation of the ERK signaling pathway as compared to Akt, and the enhanced signaling of ERK may restrain the enhancement of the Akt signaling pathway in a negative feedback manner.

The results obtained from the present study show that SHP2, MEK and PI3K inhibitors would be of potential use for the treatment of osteoporotic changes in RA patients. In particular, SHP2 inhibitors not only could inhibit the negative effect of IL-6-induced MEK/ERK and PI3K/Akt2 signaling, but also enhance the positive effect of IL-6-induced STAT3 signaling on osteoblast differentiation [37]. However, since a pro-inflammatory effect of STAT3 on synovitis has been reported [36, 58], selective inhibition of MEK2 and Akt2 signaling in osteoblasts may be more promising in order to avoid the enhancement of synovitis and consequent joint destruction.

In conclusion, our study provides new insights in the pathophysiology as well as potential treatment options for bone loss in RA, focusing on osteoblast differentiation in vitro. Our results demonstrated that IL-6 could inhibit osteoblast differentiation through MEK2/ERK and PI3K/Akt2 signaling pathways, both of which are SHP2-dependent downstream signaling pathways.

Conflict of interest All authors have no conflicts of interest.

References

1. Hashizume M, Mihara M (2011) The roles of interleukin-6 in the pathogenesis of rheumatoid arthritis. Arthritis 2011:765624
2. Ito A, Itoh Y, Sasaguri Y, Morimatsu M, Mori Y (1992) Effects of interleukin-6 on the metabolism of connective tissue components in rheumatoid synovial fibroblasts. Arthritis Rheum 35:1197–1201
3. Nishimoto N, Kishimoto T (2004) Inhibition of IL-6 for the treatment of inflammatory diseases. Curr Opin Pharmacol 4:386–391
4. De Benedetti F, Robbioni P, Massa M, Viola S, Albani S, Martini A (1992) Serum interleukin-6 levels and joint involvement in polyarticular and pauciarticular juvenile chronic arthritis. Clin Exp Rheumatol 10:493–498
5. De Benedetti F, Massa M, Pignatti P, Albani S, Novick D, Martini A (1994) Serum soluble interleukin 6 (IL-6) receptor and IL-6/soluble IL-6 receptor complex in systemic juvenile rheumatoid arthritis. J Clin Invest 93:2114–2119
6. Kotake S, Sato K, Kim KJ, Takahashi N, Udagawa N, Nakamura I, Yamaguchi A, Kishimoto T, Suda T, Kashiwazaki S (1996) Interleukin-6 and soluble interleukin-6 receptors in the synovial fluids from rheumatoid arthritis patients are responsible for osteoclast-like cell formation. J Bone Miner Res 11:88–95
7. Kwan Tat S, Padrines M, Theoleyre S, Heymann D, Fortun Y (2004) IL-6, RANKL, TNF-alpha/IL-1: interrelations in bone resorption pathophysiology. Cytokine Growth Factor Rev 15:49–60
8. Palmqvist P, Persson E, Conaway HH, Lerner UH (2002) IL-6, leukemia inhibitory factor, and oncostatin M stimulate bone resorption and regulate the expression of receptor activator of NF-kappa B ligand, osteoprotegerin, and receptor activator of NF-kappa B in mouse calvariae. J Immunol 169:3353–3362
9. Le Goff B, Blanchard F, Berthelot JM, Heymann D, Maugars Y (2010) Role for interleukin-6 in structural joint damage and systemic bone loss in rheumatoid arthritis. Joint Bone Spine 77:201–205
10. Hirano T, Matsuda T, Turner M, Miyasaka N, Buchan G, Tang B, Sato K, Shimizu M, Maini R, Feldmann M et al (1988) Excessive production of interleukin 6/B cell stimulatory factor-2 in rheumatoid arthritis. Eur J Immunol 18:1797–1801
11. Ohshima S, Saeki Y, Mima T, Sasai M, Nishioka K, Nomura S, Kopf M, Katada Y, Tanaka T, Suemura M, Kishimoto T (1998) Interleukin 6 plays a key role in the development of antigen-induced arthritis. Proc Natl Acad Sci USA 95:8222–8226
12. Dasgupta B, Corkill M, Kirkham B, Gibson T, Panayi G (1992) Serial estimation of interleukin 6 as a measure of systemic disease in rheumatoid arthritis. J Rheumatol 19:22–25
13. Poli V, Balena R, Fattori E, Markatos A, Yamamoto M, Tanaka H, Ciliberto G, Rodan GA, Costantini F (1994) Interleukin-6 deficient mice are protected from bone loss caused by estrogen depletion. EMBO J 13:1189–1196
14. Yang X, Ricciardi BF, Hernandez-Soria A, Shi Y, Pleshko Camacho N, Bostrom MP (2007) Callus mineralization and maturation are delayed during fracture healing in interleukin-6 knockout mice. Bone 41:928–936
15. Kopf M, Baumann H, Freer G, Freudenberg M, Lamers M, Kishimoto T, Zinkernagel R, Bluethmann H, Kohler G (1994) Impaired immune and acute-phase responses in interleukin-6-deficient mice. Nature 368:339–342
16. De Benedetti F, Rucci N, Del Fattore A, Peruzzi B, Paro R, Longo M, Vivarelli M, Muratori F, Berni S, Ballanti P, Ferrari S, Teti A (2006) Impaired skeletal development in interleukin-6-transgenic mice: a model for the impact of chronic inflammation on the growing skeletal system. Arthritis Rheum 54:3551–3563
17. Naka T, Nishimoto N, Kishimoto T (2002) The paradigm of IL-6: from basic science to medicine. Arthritis Res 4(Suppl 3):S233–S242
18. Wong PK, Campbell IK, Egan PJ, Ernst M, Wicks IP (2003) The role of the interleukin-6 family of cytokines in inflammatory arthritis and bone turnover. Arthritis Rheum 48:1177–1189
19. Garnero P, Thompson E, Woodworth T, Smolen JS (2010) Rapid and sustained improvement in bone and cartilage turnover markers with the anti-interleukin-6 receptor inhibitor tocilizumab plus methotrexate in rheumatoid arthritis patients with an inadequate response to methotrexate: results from a substudy of the multicenter double-blind, placebo-controlled trial of tocilizumab in inadequate responders to methotrexate alone. Arthritis Rheum 62:33–43
20. Franchimont N, Wertz S, Malaise M (2005) Interleukin-6: an osteotropic factor influencing bone formation? Bone 37:601–606
21. Li YP, Stashenko P (1992) Proinflammatory cytokines tumor necrosis factor-alpha and IL-6, but not IL-1, down-regulate the osteocalcin gene promoter. J Immunol 148:788–794
22. Peruzzi B, Cappariello A, Del Fattore A, Rucci N, De Benedetti F, Teti A (2012) c-Src and IL-6 inhibit osteoblast differentiation and integrate IGFBP5 signalling. Nat Commun 3:630
23. Hughes FJ, Howells GL (1993) Interleukin-6 inhibits bone formation in vitro. Bone Miner 21:21–28
24. Nishimura R, Moriyama K, Yasukawa K, Mundy GR, Yoneda T (1998) Combination of interleukin-6 and soluble interleukin-6 receptors induces differentiation and activation of JAK-STAT and MAP kinase pathways in MG-63 human osteoblastic cells. J Bone Miner Res 13:777–785
25. Taguchi Y, Yamamoto M, Yamate T, Lin SC, Mocharla H, DeTogni P, Nakayama N, Boyce BF, Abe E, Manolagas SC (1998) Interleukin-6-type cytokines stimulate mesenchymal progenitor differentiation toward the osteoblastic lineage. Proc Assoc Am Physicians 110:559–574
26. Ishihara K, Hirano T (2002) Molecular basis of the cell specificity of cytokine action. Biochim Biophys Acta 1592:281–296
27. Takahashi-Tezuka M, Yoshida Y, Fukada T, Ohtani T, Yamanaka Y, Nishida K, Nakajima K, Hibi M, Hirano T (1998) Gab1 acts as an adapter molecule linking the cytokine receptor gp130 to ERK mitogen-activated protein kinase. Mol Cell Biol 18:4109–4117
28. Hideshima T, Nakamura N, Chauhan D, Anderson KC (2001) Biologic sequelae of interleukin-6 induced PI3-K/Akt signaling in multiple myeloma. Oncogene 20:5991–6000
29. Tu Y, Gardner A, Lichtenstein A (2000) The phosphatidylinositol 3-kinase/AKT kinase pathway in multiple myeloma plasma cells: roles in cytokine-dependent survival and proliferative responses. Cancer Res 60:6763–6770
30. Chung TD, Yu JJ, Kong TA, Spiotto MT, Lin JM (2000) Interleukin-6 activates phosphatidylinositol-3 kinase, which inhibits apoptosis in human prostate cancer cell lines. Prostate 42:1–7
31. Qiu Y, Robinson D, Pretlow TG, Kung HJ (1998) Etk/Bmx, a tyrosine kinase with a pleckstrin-homology domain, is an effector of phosphatidylinositol 3′-kinase and is involved in interleukin 6-induced neuroendocrine differentiation of prostate cancer cells. Proc Natl Acad Sci USA 95:3644–3649
32. Chen RH, Chang MC, Su YH, Tsai YT, Kuo ML (1999) Interleukin-6 inhibits transforming growth factor-beta-induced apoptosis through the phosphatidylinositol 3-kinase/Akt and signal transducers and activators of transcription 3 pathways. J Biol Chem 274:23013–23019
33. Schmidt K, Schinke T, Haberland M, Priemel M, Schilling AF, Mueldner C, Rueger JM, Sock E, Wegner M, Amling M (2005) The high mobility group transcription factor Sox8 is a negative regulator of osteoblast differentiation. J Cell Biol 168:899–910

34. Ratisoontorn C, Seto ML, Broughton KM, Cunningham ML (2005) In vitro differentiation profile of osteoblasts derived from patients with Saethre-Chotzen syndrome. Bone 36:627–634
35. Hellmuth K, Grosskopf S, Lum CT, Wurtele M, Roder N, von Kries JP, Rosario M, Rademann J, Birchmeier W (2008) Specific inhibitors of the protein tyrosine phosphatase Shp2 identified by high-throughput docking. Proc Natl Acad Sci USA 105:7275–7280
36. Ernst M, Inglese M, Waring P, Campbell IK, Bao S, Clay FJ, Alexander WS, Wicks IP, Tarlinton DM, Novak U, Heath JK, Dunn AR (2001) Defective gp130-mediated signal transducer and activator of transcription (STAT) signaling results in degenerative joint disease, gastrointestinal ulceration, and failure of uterine implantation. J Exp Med 194:189–203
37. Itoh S, Udagawa N, Takahashi N, Yoshitake F, Narita H, Ebisu S, Ishihara K (2006) A critical role for interleukin-6 family-mediated Stat3 activation in osteoblast differentiation and bone formation. Bone 39:505–512
38. Sims NA (2004) Glycoprotein 130 regulates bone turnover and bone size by distinct downstream signaling pathways. J Clin Investig 113:379–389
39. Kawamura N, Kugimiya F, Oshima Y, Ohba S, Ikeda T et al (2007) Akt1 in osteoblasts and osteoclasts controls bone remodeling. PLoS One 2:e1058
40. Chen WS, Xu PZ, Gottlob K, Chen ML, Sokol K, Shiyanova T, Roninson I, Weng W, Suzuki R, Tobe K, Kadowaki T, Hay N (2001) Growth retardation and increased apoptosis in mice with homozygous disruption of the Akt1 gene. Genes Dev 15:2203–2208
41. Yang ZZ, Tschopp O, Hemmings-Mieszczak M, Feng J, Brodbeck D, Perentes E, Hemmings BA (2003) Protein kinase B alpha/Akt1 regulates placental development and fetal growth. J Biol Chem 278:32124–32131
42. Vandoorne K, Magland J, Plaks V, Sharir A, Zelzer E, Wehrli F, Hemmings BA, Harmelin A, Neeman M (2010) Bone vascularization and trabecular bone formation are mediated by PKB alpha/Akt1 in a gene-dosage-dependent manner: in vivo and ex vivo MRI. Magn Reson Med 64:54–64
43. Choi YH, Choi HJ, Lee KY, Oh JW (2012) Akt1 regulates phosphorylation and osteogenic activity of Dlx3. Biochem Biophys Res Commun 425:800–805
44. Mukherjee A, Rotwein P (2012) Selective signaling by Akt1 controls osteoblast differentiation and osteoblast-mediated osteoclast development. Mol Cell Biol 32:490–500
45. Mukherjee A, Wilson EM, Rotwein P (2010) Selective signaling by Akt2 promotes bone morphogenetic protein 2-mediated osteoblast differentiation. Mol Cell Biol 30:1018–1027
46. Ducy P, Desbois C, Boyce B, Pinero G, Story B, Dunstan C, Smith E, Bonadio J, Goldstein S, Gundberg C, Bradley A, Karsenty G (1996) Increased bone formation in osteocalcin-deficient mice. Nature 382:448–452
47. Higuchi C, Myoui A, Hashimoto N, Kuriyama K, Yoshioka K, Yoshikawa H, Itoh K (2002) Continuous inhibition of MAPK signaling promotes the early osteoblastic differentiation and mineralization of the extracellular matrix. J Bone Miner Res 17:1785–1794
48. Chaudhary LR, Avioli LV (2000) Extracellular-signal regulated kinase signaling pathway mediates downregulation of type I procollagen gene expression by FGF-2, PDGF-BB, and okadaic acid in osteoblastic cells. J Cell Biochem 76:354–359
49. Lin FH, Chang JB, Brigman BE (2011) Role of mitogen-activated protein kinase in osteoblast differentiation. J Orthop Res 29:204–210
50. Ge C, Xiao G, Jiang D, Franceschi RT (2007) Critical role of the extracellular signal-regulated kinase-MAPK pathway in osteoblast differentiation and skeletal development. J Cell Biol 176:709–718
51. Matsushita T, Chan YY, Kawanami A, Balmes G, Landreth GE, Murakami S (2009) Extracellular signal-regulated kinase 1 (ERK1) and ERK2 play essential roles in osteoblast differentiation and in supporting osteoclastogenesis. Mol Cell Biol 29:5843–5857
52. Schindeler A, Little DG (2006) Ras-MAPK signaling in osteogenic differentiation: friend or foe? J Bone Miner Res 21:1331–1338
53. Sims NA, Jenkins BJ, Quinn JM, Nakamura A, Glatt M, Gillespie MT, Ernst M, Martin TJ (2004) Glycoprotein 130 regulates bone turnover and bone size by distinct downstream signaling pathways. J Clin Invest 113:379–389
54. Duplomb L, Baud'huin M, Charrier C, Berreur M, Trichet V, Blanchard F, Heymann D (2008) Interleukin-6 inhibits receptor activator of nuclear factor kappaB ligand-induced osteoclastogenesis by diverting cells into the macrophage lineage: key role of Serine727 phosphorylation of signal transducer and activator of transcription 3. Endocrinology 149:3688–3697
55. Yamanaka Y, Nakajima K, Fukada T, Hibi M, Hirano T (1996) Differentiation and growth arrest signals are generated through the cytoplasmic region of gp130 that is essential for Stat3 activation. EMBO J 15:1557–1565
56. Nakajima K, Yamanaka Y, Nakae K, Kojima H, Ichiba M, Kiuchi N, Kitaoka T, Fukada T, Hibi M, Hirano T (1996) A central role for Stat3 in IL-6-induced regulation of growth and differentiation in M1 leukemia cells. EMBO J 15:3651–3658
57. Hirano T, Matsuda T, Nakajima K (1994) Signal transduction through gp130 that is shared among the receptors for the interleukin 6 related cytokine subfamily. Stem Cells 12:262–277
58. Krause A, Scaletta N, Ji JD, Ivashkiv LB (2002) Rheumatoid arthritis synoviocyte survival is dependent on Stat3. J Immunol 169:6610–6616

Effect of Intermittent Administration of Teriparatide (Parathyroid Hormone 1-34) on Bone Morphogenetic Protein-Induced Bone Formation in a Rat Model of Spinal Fusion

Tokimitsu Morimoto, MD, Takashi Kaito, MD, PhD, Masafumi Kashii, MD, PhD, Yohei Matsuo, MD, Tsuyoshi Sugiura, MD, Motoki Iwasaki, MD, and Hideki Yoshikawa, MD, PhD

Investigation performed at the Departments of Orthopedic Surgery and Orthopedic Biomaterial Science, Graduate School of Medicine, Osaka University, Osaka, Japan

Background: Although clinical bone morphogenetic protein (BMP) therapy is effective at enhancing bone formation in patients managed with spinal arthrodesis, the required doses are very high. Teriparatide (parathyroid hormone 1-34) is approved by the U.S. Food and Drug Administration to treat osteoporosis and is a potent anabolic agent. In this study, intermittent administration of parathyroid hormone 1-34 combined with transplantation of BMP was performed to elucidate the effect of parathyroid hormone 1-34 on the fusion rate and quality of newly formed bone in a rat model.

Methods: A total of forty-eight male Sprague-Dawley rats underwent posterolateral lumbar spinal arthrodesis with one of three different treatments with recombinant human (rh) BMP-2: (1) 0 μg (control), (2) 2 μg (low dose), or (3) 50 μg (high dose). Each of the rhBMP-2 treatments was studied in combination with intermittent injections of either parathyroid hormone 1-34 (180 μg/kg/wk) or saline solution starting two weeks before the operation and continuing until six weeks after the operation. Osseous fusion was assessed with use of radiographs and a manual palpation test. Microstructural indices of the newly formed bone were evaluated with use of micro-computed tomography. The serum markers of bone metabolism were also quantified.

Results: The fusion rate in the group treated with 2 μg of rhBMP-2 significantly increased (from 57% to 100%) with the administration of parathyroid hormone 1-34 ($p < 0.05$). The fusion rates in the other groups did not change significantly with the administration of parathyroid hormone 1-34. The bone volume density of the newly formed bone significantly increased in both the 2-μg and 50-μg rhBMP-2 treatment groups with the administration of parathyroid hormone 1-34 ($p < 0.01$). Micro-computed tomography scans of the newly formed bone clearly demonstrated an abundance of trabecular bone formation in the group treated with parathyroid hormone 1-34. In addition, serum levels of osteocalcin were significantly increased in the parathyroid hormone 1-34 treatment group.

Conclusions: Intermittent administration of parathyroid hormone 1-34 significantly increased fusion rates in the group treated with low-dose rhBMP-2, and it improved the quality of the newly formed bone in both the high and low-dose groups in a rat model of rhBMP-2-induced spinal fusion.

Clinical Relevance: Our results suggest that the combined administration of rhBMP-2 and parathyroid hormone 1-34 may lead to efficient bone regeneration.

Peer Review: This article was reviewed by the Editor-in-Chief and one Deputy Editor, and it underwent blinded review by two or more outside experts. It was also reviewed by an expert in methodology and statistics. The Deputy Editor reviewed each revision of the article, and it underwent a final review by the Editor-in-Chief prior to publication. Final corrections and clarifications occurred during one or more exchanges between the author(s) and copyeditors.

Disclosure: One or more of the authors received payments or services, either directly or indirectly (i.e., via his or her institution), from a third party in support of an aspect of this work. None of the authors, or their institution(s), have had any financial relationship, in the thirty-six months prior to submission of this work, with any entity in the biomedical arena that could be perceived to influence or have the potential to influence what is written in this work. Also, no author has had any other relationships, or has engaged in any other activities, that could be perceived to influence or have the potential to influence what is written in this work. The complete **Disclosures of Potential Conflicts of Interest** submitted by authors are always provided with the online version of the article.

Autogenous bone-grafting is the current gold standard for achieving spinal fusion. However, its use is limited by the amount of bone available and by the associated donor-site morbidity[1,2]. Moreover, the rate of pseudarthrosis has been reported to range between 5% and 43%[3,4]. These problems have prompted surgeons to identify alternative means for stimulating bone formation.

One possibility is the use of bone morphogenetic proteins (BMPs), which are a group of growth factors belonging to the transforming growth factor superfamily that are known to elicit new bone formation[5-7]. However, the uncontrolled release of high concentrations of BMPs can cause inflammation, soft-tissue edema, and unintended bone formation[8,9]. Thus, the U.S. Food and Drug Administration has approved the use of BMPs in the spine for anterior lumbar spinal arthrodesis only; uses for posterior spinal arthrodesis have been "off label." Therefore, an efficient method for reducing the required dose of BMPs by enhancing the bioactivity is required.

Teriparatide (recombinant human parathyroid hormone [PTH] 1-34) is the only anabolic agent that has been approved by the U.S. Food and Drug Administration for the treatment of osteoporosis[10,11]. Intermittent administration of PTH 1-34 results in osteoblastic proliferation and differentiation, thereby leading to an increase in bone mass[12-14]. Recently, upregulation and modulation of BMP signaling by PTH have been reported[15,16]. These mechanisms indicate the possibility of synergistic bone regeneration by the co-administration of rhBMP-2 and PTH 1-34.

In the present study, intermittent administration of PTH 1-34 combined with BMP transplantation was performed to elucidate the effect of PTH 1-34 on the fusion rate and quality of the newly formed bone in a rat model of spinal fusion.

Materials and Methods

Experimental Design

A total of four dozen eight-week-old male Sprague-Dawley rats (weight, 270 to 290 g) were used. The animals were allocated to one of six different treatment groups by assigning one of three surgical treatments and one of two injection treatments to each rat. Each treatment group consisted of eight animals (see Appendix). The three surgical treatments consisted of (1) implantation of a collagen-only carrier (Groups A and B), (2) implantation of a collagen carrier loaded with 2 μg of rhBMP-2 (Groups C and D), and (3) implantation of a collagen carrier loaded with 50 μg of rhBMP-2 (Groups E and F). The animals in each treatment group were further divided into two subgroups, including rats that also received either (1) injections of PTH 1-34 (Groups B, D, and F) or (2) injections of saline solution (Groups A, C, and E) (see Appendix). rhBMP-2 doses for the low and high-dose groups were based on a preliminary spinal fusion study (data not shown). We chose 2 μg (fusion rate, 50%; concentration, 20 μg/mL) as the low dose because this amount of rhBMP-2 is better suited for elucidating the effect of PTH 1-34 on the fusion rate, and we chose 50 μg (fusion rate, 100%; concentration, 500 μg/mL) as the high dose because this amount of rhBMP-2 reflects the clinical use of high-dose (1500-μg/mL) rhBMP-2.

Injections of PTH 1-34

Rats in the control group were given subcutaneous injections of 0.9% saline solution, whereas rats in the PTH groups were given subcutaneous injections of PTH 1-34 (60 μg/kg) three times a week (total, 180 μg/kg/wk). Injections were initiated two weeks prior to surgery and were continued for six weeks after surgery, at which time the animals were killed.

TABLE I Results of Radiographic Analysis of Spinal Fusion

	Injected Material* (%)	
rhBMP-2 Dosage (μg)	Saline Solution	PTH 1-34
0	0 of 8 (0)	0 of 8 (0)
2	4 of 7 (57)	8 of 8 (100)†
50	7 of 8 (88)	8 of 8 (100)

*The values are given as the number of spines that were found to have successfully fused as assessed with radiographs, with the percentage in parentheses. †At this dosage, the rate of fusion was significantly higher in the group that received PTH 1-34 ($p < 0.05$).

Posterior Spinal Fusion

Preparation of a Collagen Carrier Vehicle

A commercially available absorbable collagen sponge (CollaCote; Integra LifeSciences, Plainsboro, New Jersey) was cut into 5 × 10-mm fragments. Thereafter, the appropriate concentration of rhBMP-2 (0, 2, or 50 μg) was dissolved in phosphate buffered saline solution and applied to the carrier just before implantation.

Surgical Technique of L4-L5 Posterolateral Spinal Arthrodesis

All of the animal procedures were conducted in accordance with the guidelines of the Regulations on Animal Experimentation at Osaka University. The rats were anesthetized with a combination of 0.15 mg/kg of medetomidine (Domitor; Nippon Zenyaku Kogyo, Fukushima, Japan), 2 mg/kg of midazolam (Dormicum; Astellas Pharma, Tokyo, Japan), and 2.5 mg/kg of butorphanol (Vetorphale; Meiji Seika, Tokyo, Japan). As per the usual method[16,17], a posterior midline skin incision was made, followed by two separate paramedian incisions in the lumbar fascia 3 mm from the midline, through which the transverse processes were exposed. The L4 and L5 transverse processes were decorticated with use of a high-speed burr. Subsequently, a collagen sponge containing 0, 2, or 50 μg of rhBMP-2 was implanted on each side. The rats were housed in separate cages and allowed to eat and drink ad libitum while their condition was monitored daily.

Euthanasia and Analyses

Just prior to euthanization of the animals, blood samples were collected and stored at −80°C until the serum markers of bone metabolism were analyzed. The rats were killed with an overdose of anesthetics at six weeks after surgery. The spinal segments and femora were harvested and fixed with 10% formalin.

Assessment of Fusion

Radiographic Assessment

Fusion between L4 and L5 was evaluated with radiographs made with use of an MX-20 Specimen Radiography System (Faxitron X-Ray, Lincolnshire, Illinois) under consistent conditions (35 kV, 300 μA, 300 seconds). Fusion was considered to have occurred when there was clear evidence of new bone formation and osseous bridging with cortical continuity between the L4 and L5 transverse processes.

Manual Assessment

The explanted lumbar spines were manually tested for intersegmental motion. Any motion detected on either side between the facets or between the transverse processes was considered to be a failure of fusion.

In both assessments, the spines were scored as either fused or not fused independently by three examiners. The L4-L5 segments were considered to be fused only when all three observers agreed.

TABLE II Results of Spinal Fusion as Assessed with Manual Palpation

	Injected Material* (%)	
rhBMP-2 Dosage (μg)	Saline Solution	PTH 1-34
0	0 of 8 (0)	0 of 8 (0)
2	2 of 7 (29)	8 of 8 (100)†
50	8 of 8 (100)	8 of 8 (100)

*The values are given as the number of spines that were found to have successfully fused as assessed with manual palpation, with the percentage in parentheses. †At this dosage, the rate of fusion was significantly higher in the group that received PTH 1-34 ($p < 0.05$).

Micro-Computed Tomography Analysis

Following manual evaluation, the spines were scanned with use of high-resolution micro-computed tomography (micro-CT) (R_mCT; Rigaku Mechatronics, Tokyo, Japan); each sample was scanned twice. The micro-CT data were collected at 90 kV and 200 μA. Visualization and data reconstruction were performed with use of TRI/3D-BON software (RATOC System Engineering, Tokyo, Japan).

Analysis of the Microstructural Indices of the Newly Formed Fusion Mass

The quality of the newly formed fusion mass between the transverse processes where bone did not originally exist was analyzed as described previously[18] (see Appendix). Scanning of the newly formed bone was initiated from the lower end plate level of the L4 vertebral body and continued cranially in 2.0-mm increments (fifty slices) at a resolution of 40 μm per voxel. Bone volume density, trabecular thickness, trabecular number, trabecular separation, thickness of cortical bone, and cortical bone ratio were estimated. The bone volume density corresponds to the ratio of bone volume to fusion-mass volume.

Microstructural Analysis of the Fused Spinal Segments

The tissue volume and bone volume of the total fusion mass were measured (from the bottom to 15 mm cranially from the bottom of the L5 transverse process, for a total of 254 slices) at a resolution of 59 μm per voxel.

Analysis of the Systemic Effects of PTH 1-34

To evaluate the systemic effects of PTH 1-34, the bone volume density of the distal femoral epiphysis and L6 vertebral body was analyzed at a resolution of 40 μm per voxel. Scanning of the distal part of the femur was initiated at 1.5 mm proximal to the growth plate and continued at 3.0-mm increments (for a total of seventy-five slices). Scanning of the L6 vertebral body was initiated at 1.0 mm cranial to the lower growth plate and continued at 3.2-mm increments (for a total of eighty slices).

Analysis of Serum Markers of Bone Metabolism

Serum markers of bone metabolism were analyzed with use of an enzyme-linked immunosorbent assay specific for osteocalcin (Osteocalcin High Sensitive EIA kit [rat]; Takara Bio, Shiga, Japan), type-I collagen cross-linked C-telopeptides (RatLaps ELISA; Immunodiagnostic Systems, Fountain Hills, Arizona), and tartrate-resistant acid phosphatase-5b (RatTRAP Assay; Immunodiagnostic Systems), according to the manufacturer's instructions. Serum from all animals ($n = 47$) was measured once for each marker, with comparisons performed between the groups treated with PTH 1-34 (Groups B, D, and F) and those treated with saline solution (Groups A, C, and E).

Histologic Analysis

The dissected and formalin-fixed spines were demineralized with 50% formic acid and 10% sodium citrate, dehydrated in a graded ethanol series, and

TABLE III Microstructural Indices of Newly Formed Bone

		Injected Material*	
Parameter	rhBMP-2 Dosage (μg)	Saline Solution	PTH 1-34
Tissue volume (mm^3)	2	5.5 ± 5.4	17.1 ± 13.3†
	50	34.8 ± 22.2	29.1 ± 12.0
Bone volume (mm^3)	2	0.7 ± 0.9	3.8 ± 3.2†
	50	2.3 ± 2.7	6.3 ± 2.8†
Bone volume density (%)	2	12.1 ± 5.2	22.1 ± 5.5†
	50	7.1 ± 4.6	22.2 ± 5.5†
Trabecular thickness (μm)	2	142.6 ± 15.1	166.8 ± 31.1‡
	50	153.0 ± 35.9	181.8 ± 17.2†
Trabecular number (mm^{-1})	2	0.8 ± 0.8	0.7 ± 0.2
	50	0.3 ± 0.2	0.6 ± 0.2†
Trabecular separation (μm)	2	305.5 ± 97.2	268.9 ± 56.4
	50	756.9 ± 428.7	298.7 ± 64.9†
Cortical bone ratio (%)	2	41.5 ± 7.6	39.4 ± 11.0
	50	28.8 ± 17.1	30.1 ± 4.8‡
Cortical bone thickness (μm)	2	313.2 ± 77.4	391.3 ± 90.8†
	50	272.4 ± 109.5	365.1 ± 53.0†

*Values are given as the mean and the standard deviation. †At this dosage, the value was significantly higher in the group that received PTH 1-34 ($p < 0.01$). ‡At this dosage, the value was significantly higher in the group that received PTH 1-34 ($p < 0.05$).

embedded in paraffin wax. Serial coronal sections (thickness, 5 μm) of the involved segments were cut and stained with hematoxylin and eosin.

Statistical Analysis

The PASW Statistics computer software program (version 18.0, SPSS, Chicago, Illinois) was used for all of the analyses. The Mann-Whitney U test was used for the comparison of microstructural indices and serum markers of bone metabolism. The chi-square test was used for the comparison of fusion assessments. In all analyses, the level of significance was set at $p < 0.05$.

Source of Funding

This work was supported by a Grant-in-Aid for Scientific Research from the Japan Society for the Promotion of Science (JSPS KAKENHI Grant 25861313).

Results

Spinal Fusion

Radiographic Analysis

One rat in Group C died the day after surgery; thus, a total of forty-seven rats were used for the final analysis. Fusion at L4-L5 in the groups treated with 2 μg of rhBMP-2 significantly increased, from four of seven (57%) to eight of eight (100%), with the administration of PTH 1-34 ($p < 0.05$). Fusion in the groups treated with 0 or 50 μg of rhBMP-2 did not change significantly with the administration of PTH 1-34 (in both groups treated with 0 μg of rhBMP-2, fusion occurred in zero of eight [0%] spines regardless of whether PTH 1-34 was used; in the groups treated with 50 μg of rhBMP-2, fusion increased from seven of eight [88%] to eight of eight [100%] with the use of PTH 1-34) (Table I).

Manual Assessment

All the spines in Groups E and F, which were treated with 50 μg of rhBMP-2, were assessed with manual palpation and were considered to have fused (eight of eight in each group, 100%). None of the spines in Groups A or B, which were treated with 0 μg of rhBMP-2, were considered to have fused (zero of eight in each group, 0%). Fusion in the spines that were treated with

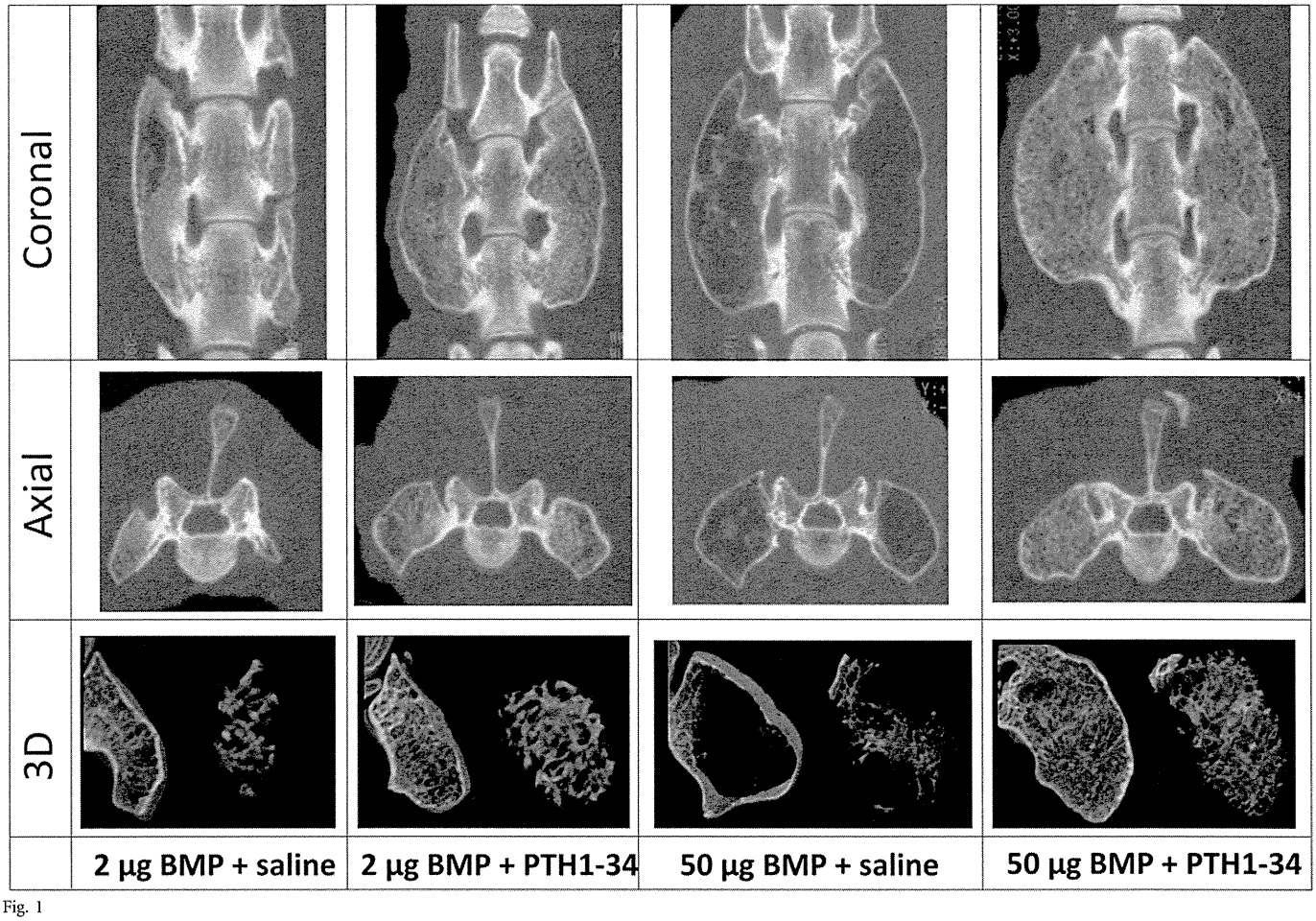

Fig. 1

In the groups treated with 2 μg of recombinant human bone morphogenetic protein (BMP)-2, the administration of teriparatide (parathyroid hormone [PTH] 1-34) improved osseous bridging between the transverse processes, the volume of the fusion mass, and the trabecular bone volume inside the fusion mass. In the group treated with 50 μg of rhBMP-2 and saline solution, the induced fusion mass resembled an eggshell (a thin outer layer of cortical bone with scarce trabecular bone inside). PTH 1-34 administration with 50-μg rhBMP-2 treatment resulted in the formation of a fusion mass that was completely filled with thick trabecular bone. 3D = three-dimensional.

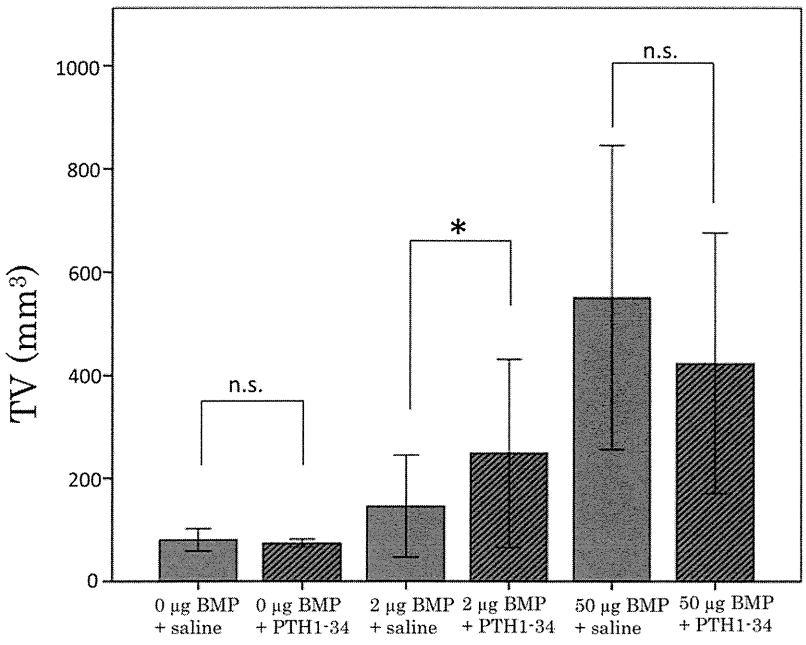

Fig. 2

Teriparatide (parathyroid hormone [PTH] 1-34) administration did not change the tissue volume (TV) in the 0-μg bone morphogenetic protein (BMP) groups. In the groups treated with 2 μg of rhBMP-2, PTH 1-34 administration significantly increased the tissue volume (TV) ($p < 0.05$). In the 50-μg rhBMP-2 groups, PTH 1-34 administration showed a decreasing trend; however, it was not significant (n.s.). The asterisk indicates a significant difference in tissue volume.

2 μg of rhBMP-2 increased from two of seven (29%, Group C) to eight of eight (100%, Group D) with the administration of PTH 1-34 ($p < 0.01$) (Table II).

Micro-CT Analysis

Analysis of the Microstructural Indices of the Fused Spinal Segments

The specimens treated with 2 or 50 μg of rhBMP-2 (Groups C, D, E, and F) were used for this analysis, because the specimens treated with 0 μg of rhBMP-2 (Groups A and B) showed little or no new bone formation.

The trabecular bone volume and structural parameters (bone volume, bone volume density, and trabecular thickness) in the groups treated with 2 μg or 50 μg of rhBMP-2 were significantly increased with the administration of PTH 1-34, and the trabecular number in the group treated with 50 μg of rhBMP-2 was also significantly increased with PTH 1-34 administration ($p < 0.01$). The cortical bone parameters of the groups treated with 2 μg or 50 μg of rhBMP-2 were also increased with the administration of PTH 1-34. Interestingly, the tissue volume in the group treated with 50 μg of rhBMP-2 decreased with the use of PTH 1-34, although the tissue volume in the groups treated with 2 μg of rhBMP-2 was significantly increased with the use of PTH 1-34 (Table III). Micro-CT coronal and axial two-dimensional images and reconstructed three-dimensional images of the newly formed bone clearly demonstrated abundant trabecular bone formation in the groups treated with PTH 1-34 (Fig. 1).

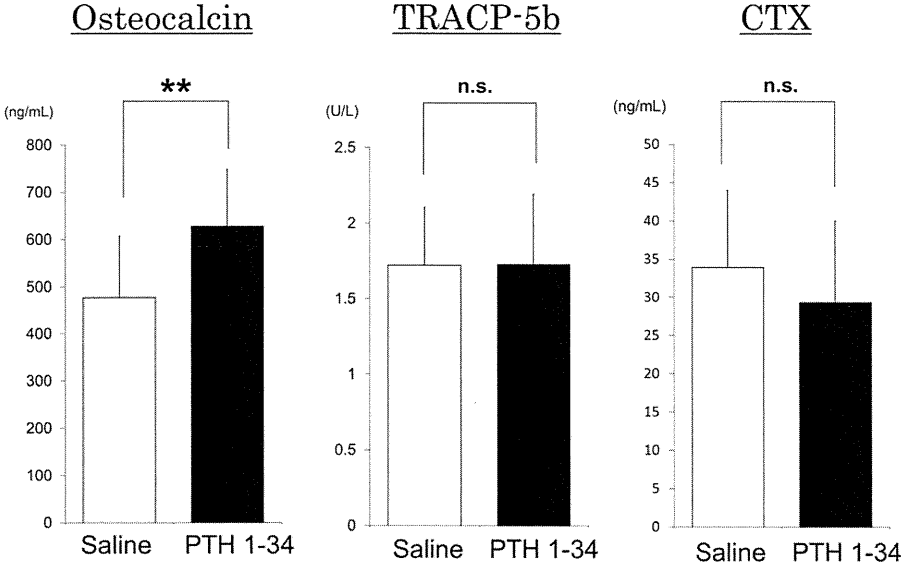

Fig. 3

Osteocalcin (bone-formation marker) levels were significantly increased with the administration of teriparatide (parathyroid hormone [PTH] 1-34) ($p < 0.01$), but tartrate-resistant acid phosphatase (TRACP)-5b (bone-resorption marker) and type-I collagen cross-linked C-telopeptides (CTX) (bone-resorption marker) levels were not significantly altered (n.s.). The double asterisk indicates a significant difference in tissue volume.

Microstructural Analysis of the Fused Spinal Segments

The mean bone volume density (and standard deviation) in Groups A and B, which received 0 μg, was 18.5% ± 3.5% and 27.8% ± 7.4% ($p < 0.01$), respectively. In Groups C and D, which received 2 μg, it was 19.6% ± 3.4% and 23.4% ± 4.8% ($p < 0.05$), respectively. In Groups E and F, which received 50 μg, it was 13.7% ± 4.2% and 24.2% ± 6.0% ($p < 0.01$), respectively. However, the alterations in tissue volume values caused by PTH 1-34 use differed in each group. The tissue volume between the groups treated with 0 μg of rhBMP-2 with or without PTH 1-34 did not differ significantly (Group A, 79.8 ± 10.2 mm^3; Group B, 72.4 ± 5.1 mm^3; $p = 0.14$). The tissue volume in the groups treated with 2 μg of rhBMP-2 significantly increased with the use of PTH 1-34 (Group C, 145.4 ± 49.6 mm^3; Group D, 239.1 ± 88.6 mm^3; $p < 0.05$); the tissue volume in the groups treated with 50 μg of rhBMP-2 decreased with the use of PTH 1-34, although the change was not significant (Group E, 469.1 ± 207.0 mm^3; Group F, 397.3 ± 137.8 mm^3; $p = 0.44$) (Fig. 2). The effect of PTH 1-34 use on tissue volume was anabolic in the 2-μg BMP group and was catabolic in the 50-μg BMP group.

Analysis of the Effect of PTH Administration on the Adjacent Vertebra (L6) and Femur

The bone volume densities of both the distal femoral epiphysis and the L6 vertebral body were significantly increased with the use of PTH 1-34 compared with those treated without PTH 1-34 (femur: 18.5% ± 10.3% compared with 49.4% ± 14.1%, $p < 0.001$; L6 vertebra: 26.1% ± 10.4% compared with 37.7% ± 4.2%, $p < 0.001$). The bone volume density of both the femur and the L6 vertebra did not differ based on the dosage of rhBMP-2.

Analysis of Serum Markers of Bone Metabolism

Enzyme-linked immunosorbent assay demonstrated that serum levels of osteocalcin were significantly higher in the groups treated with PTH 1-34 compared with those treated with saline solution ($p < 0.01$), whereas no differences were observed in serum levels of type-I collagen cross-linked C-telopeptides and tartrate-resistant acid phosphatase-5b between the groups treated with saline solution and those treated with PTH 1-34 (Fig. 3).

Histologic Analysis

Microscopic evaluation of the coronal sections of the treated spinal segments demonstrated that the groups treated with 0 μg of rhBMP-2 (Groups A and B) showed minimal evidence of new bone, and no apparent difference was noted with regard to PTH 1-34 administration (Figs. 4-A and 4-B). In the Group C rats treated with 2 μg of rhBMP-2 and injections of saline solution, the fusion mass between the L4-L5 transverse processes was discontinuous or separated by cartilage tissue (Fig. 4-C). However, in the group with the same 2-μg rhBMP-2 dosage (Group D), the addition of PTH 1-34 clearly improved the osseous continuity between the transverse processes and increased the volume of the fusion mass (Fig. 4-D). In the groups treated with 50 μg of rhBMP-2, a huge fusion mass was found even in the group that received saline solution injections (Group E); however, a majority of the newly formed fusion masses in Group E comprised fatty marrow within thin, eggshell-like cortical bone (Fig. 4-E). PTH 1-34 markedly increased the number and thickness of trabecular bone in the fusion mass (Fig. 4-F).

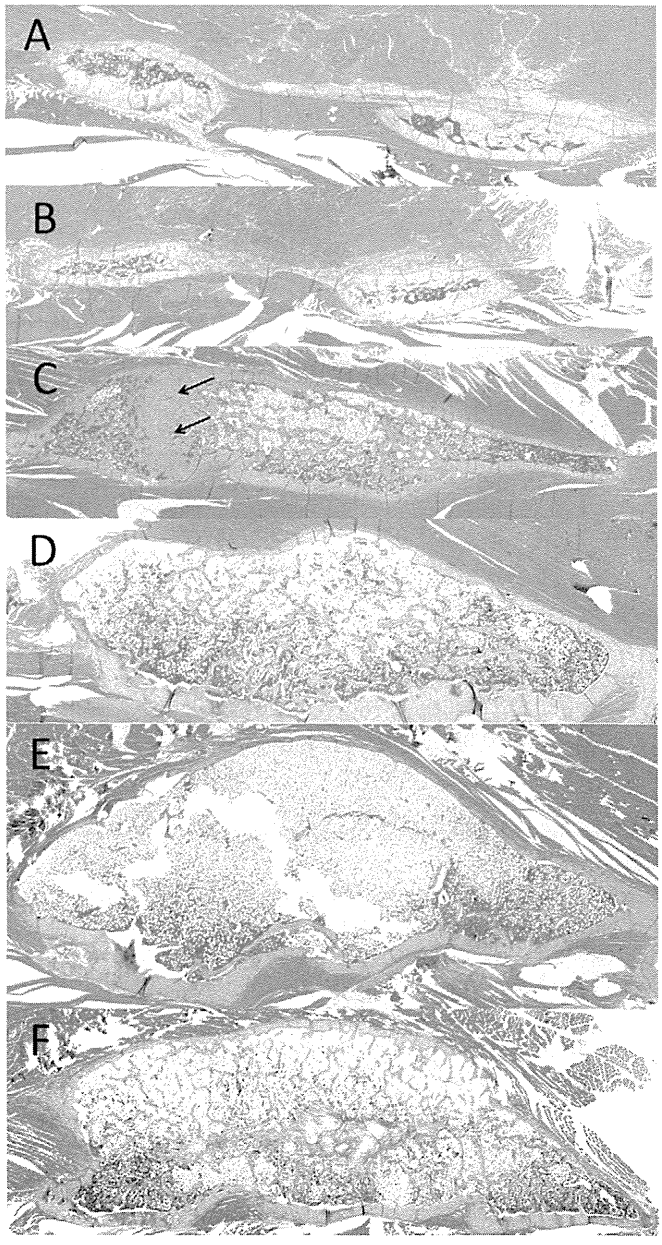

Fig. 4

Low-power photomicrographs (magnification, ×0.5). Coronal sections of the L4-L5 transverse processes of the spines of rats from Group A (Fig. 4-A) and Group B (Fig. 4-B) demonstrate no evidence of bone formation between the transverse processes. Cross-section of the transverse processes of rats from Group C (Fig. 4-C) show fibrocartilaginous union (arrows). In Group D, PTH 1-34 administration clearly improved the osseous continuity and the bone volume of the fusion mass (Fig. 4-D). In Group E (50 μg of rhBMP-2), a huge fusion mass was found; however, the fusion mass comprised fatty marrow within thin, eggshell-like cortical bone (Fig. 4-E). In Group F, PTH 1-34 administration markedly increased the number and thickness of trabecular bone in the fusion mass (Fig. 4-F).